Electronic Supplementary Material (ESI) for ChemComm.

Supporting Information

The Diverse Reactivity of $NOBF_4$ towards Silylene, Disilene, Germylene and Stannylene

Nasrina Parvin,[a] Nilanjana Sen,[a] Puthan Veetil Muhasina,[b] Srinu Tothadi,[c] Pattiyil Parameswaran,*[b] and Shabana Khan*[a]

Contents

S1. Experimental Details:

All experiments were carried out under an atmosphere of dry argon or in vaccuo using standard Schlenk technique and in a dinitrogen filled MBRAUN MB 150-G1 glovebox. The solvents used were purified by MBRAUN solvent purification system MB SPS-800. $NOBF_4$ was purchased from the Sigma-Aldrich and used without further purification. **1**, **2**, **7**, **9**, $Cp^*{}_2Ge$, IPr and $Cp^*SiN(TMS)_2{=}SiN(TMS)_2Cp^*$ were prepared by the literature method.[S1] ^1H, ^{13}C, ^{29}Si, ^{11}B and ^{19}F NMR spectra were recorded with Bruker 400 MHz spectrometer, using $CDCl_3$ as solvent with an external standard ($SiMe_4$ for ^1H, ^{13}C, ^{29}Si and CHF_3 for ^{19}F). Concentrated solution of the samples in C_6D_6 were sealed off in a NMR tube for measurement. Mass spectra were recorded using AB Sciex, 4800 plus MALDI TOF/TOF.

Synthesis of 3 and 5:

30 mL toluene was added into the mixture of **1** (E= Si) (0.210g, 0.5 mmol) and $NOBF_4$ (0.058g, 0.5 mmol) in a 100 mL Schlenk flask. After 30h stirring at room temperature, the pale yellow colored solution was filtered off and the volume was reduced to 15 mL and kept it at 0 °C. The colorless crystals of **3** and **5** suitable for X-ray analysis was obatined wthin 24h. It must be noted here that the crystals of **3** and **5** grow under the same condition and it was not possible to separate them via fractional crystallization in the first crop, although **3** comes as a major product (0.12 g, 26%). For the same reason it was difficult to get a pure NMR of only **3**. In the second fraction, only **5** crsyallizes (0.08 g, 17%).

3: ^1H NMR (400 MHz, $CDCl_3$, 298K): δ 0.39 (*s*, 18H, Si*Me₃*), 0.66 (*s*, 18H, Si*Me₃*), 1.25 (*s*, 36H, C*Me₃*), 6.95-6.99 (*m*, 3H, Ph), 7.02-7.06 (*m*, 2H, Ph), 7.15-7.18 (*m*, 3H, Ph), 7.26 (*s*, 2H, Ph) ppm. $^{13}C\{^1H\}$ NMR (100.613 MHz, $CDCl_3$, 298 K): δ 1.02 (Si*Me₃*), 4.79 (Si*Me₃*), 30.72 (*C*Me₃), 31.20 (*C*Me₃), 53.86 (C*Me₃*), 57.09 (C*Me₃*), 126.87, 127.83, 128.17, 128.38, 129.62, 130.01, 132.47, 133.01(Ph-*C*), 166.54 (N*C*N) ppm. $^{29}Si\{^1H\}$ NMR (79.495 MHz, $CDCl_3$, 298 K): δ 9.52, 0.87, -13.39, -24.99, 61.52 (*d*, $J_{Si\text{-}F}$= 233.5Hz). $^{19}F\{^1H\}$ NMR (376.49 MHz, $CDCl_3$, 298): δ -109.66 and -148.75 ppm. $^{11}B\{^1H\}$ NMR (128.387 MHz, $CDCl_3$, 298 K): δ -0.84 (*s*), 3.02 (*m*) MALDI: *m/z* [$C_{21}H_{41}N_3Si_3OBF_3$]: 485.07 [M-F]; *m/z* [$C_{21}H_{41}N_3Si_3F_2$]: 387.39 [M-$SiMe_3$].

5: ^1H NMR (400 MHz, $CDCl_3$, 298K): δ 0.32 (*s*, 18H, Si*Me₃*), 1.10 (*s*, 36H, C*Me₃*), 7.33-7.37 (*m*, 2H, Ph), 7.39-7.47 (*m*, 3H, Ph) ppm. $^{13}C\{^1H\}$ NMR (100.613 MHz, $CDCl_3$, 298 K): δ 1.03 (Si*Me₃*), 4.80 (Si*Me*$_3$), 31.21 (*C*Me$_3$), 53.86 (C*Me*$_3$), 127.83, 128.18, 129.92, 133.03 (Ph-*C*), 174.03 (N*C*N) ppm. ^{19}F{^{1}H} NMR (376.49 MHz, CDCl$_3$, 298): *δ* -109.66.

Synthesis of 4 and 6:

30 mL toluene was added into the mixture of **2** (E= Ge) (0.232g, 0.5 mmol) and NOBF$_4$ (0.058g, 0.5 mmol) in a 100 mL Schlenk flask. After 24h stirring at room temperature, the reaction mixture was filtered and concentrated. The colorless crystals suitable for X-ray analysis were obatined wthin 24 hrs at 0 °C. Similar to the previous case, the crystals of **4** and **6** grow under the same condition and it was not possible to separate them via fractional crystallization in the first crop, although **4** comes as a major product (0.12 g, 23%). For the same reason it was difficult to get a pure NMR of only **4**. In the second fraction, only **6** crsyallizes (0.09 g, 19%).

4: ^{1}H NMR (400 MHz, CDCl$_3$, 298K): *δ* 0.52-0.56 (*m*, 36H, Si*Me*$_3$), 1.10-1.13 (*m*, 36H, C*Me*$_3$), 6.83-6.87 (*m*, 2H, Ph), 7.00-7.05 (*m*, 3H, Ph), 7.15 (*m*, 4H, Ph), 7.68-7.71 (*s*, 1H, Ph) ppm. ^{13}C{^{1}H} NMR (100.613 MHz, CDCl$_3$, 298 K): *δ* 2.74 (Si*Me*$_3$), 3.29 (Si*Me*$_3$), 3.29 (Si*Me*$_3$), 3.80 (Si*Me*$_3$), 4.21 (Si*Me*$_3$), 4.73 (Si*Me*$_3$), 29.30 (*C*Me$_3$), 29.79 (*C*Me$_3$), 30.37 (C*Me*$_3$), 31.03 (C*Me*$_3$), 52.60 (C*Me*$_3$), 53.90 (C*Me*$_3$), 55.54 (C*Me*$_3$), 126.33, 127.37, 127.68, 127.87, 128.17, 128.63, 129.95, 131.34, 135.09 (Ph-*C*), 169.71(N*C*N), 175.97 (N*C*N) ppm. ^{29}Si{^{1}H} NMR (79.495 MHz, CDCl$_3$, 298 K): *δ* 11.40 (*Si*Me$_3$), 4.21 (*Si*Me$_3$), 2.33 (*Si*Me$_3$) ppm. ^{19}F{^{1}H} NMR (376.49 MHz, CDCl$_3$, 298): *δ* -105.68 and -142.56 ppm. ^{11}B{^{1}H} NMR (128.387 MHz, CDCl$_3$, 298 K): *δ* -0.14 (*dd,* $J_{B\text{-}F}$= 22.4, 11.2 *Hz*) MALDI: *m/z* [$C_{21}H_{41}N_3Si_2GeOBF_3$]: 511.41 [M-2F]$^+$.

6: ^{1}H NMR (400 MHz, CDCl$_3$, 298K): *δ* 0.53 (*s*, 18H, Si*Me*$_3$), 1.10 (*s*, 18H, C*Me*$_3$), 6.82-6.89 (*m*, 2H, Ph), 6.96-6.98 (*m*, 1H, Ph), 7.12 (*s*, 2H, Ph) ppm. ^{19}F{^{1}H} NMR (376.49 MHz, CDCl$_3$, 298): *δ* -105.68 ppm.

Synthesis of 8:

30 mL toluene was added into the mixture of **7** (E= Sn) (0.255g, 0.5 mmol) and NOBF$_4$ (0.058g, 0.5 mmol) in a 100 mL Schlenk flask. After 24h stirring at room temperature, the solution was filtered through frit. Colorless crystals were obtained upon supersaturation. Yield: 0.110 g (40%). ^{1}H NMR (400 MHz, CDCl$_3$, 298K): *δ* 0.26-0.32 (*m*, 18H, Si*Me*$_3$), 1.04-1.07 (*m*, 18H, C*Me*$_3$), 7.20-7.25 (*m*, 1H, Ph), 7.32-7.40 (*m*, 4H, Ph) ppm. ^{13}C{^{1}H} NMR (100.613 MHz, CDCl$_3$, 298 K): *δ* 4.43 (Si*Me*$_3$), 4.86 (Si*Me*$_3$), 31.96 (*C*Me$_3$), 32.12 (C*Me*$_3$), 32.27 (C*Me*$_3$), 55.69 (C*Me*$_3$), 127.67, 127.84, 128.34, 128.65, 129.24, 129.79, (Ph-*C*), 169.03 (N*C*N) ppm. ^{29}Si{^{1}H} NMR (79.495 MHz, CDCl$_3$, 298 K): *δ* 4.35 (*Si*Me$_3$), 4.69 (*Si*Me$_3$) ppm. ^{119}Sn{^{1}H} NMR (149.18MHz, CDCl$_3$, 298): *δ*

-387.33 (*d*, $J_{Sn\text{-}F}$=2984.8 Hz) ppm. $^{19}F\{^{1}H\}$ NMR (376.49 MHz, $CDCl_3$, 298): δ -94.92 and -137.83 ppm. HRMS: *m/z* [$C_{21}H_{41}N_3Si_2SnF_2$]: 572.16 [M+Na]$^+$.

Synthesis of 10:

9 (0.300 g, 0.422 mmol) and $NOBF_4$ (0.098 g, 0.844 mmol) were taken in 1:2 equivalent in a 100 mL Schlenk flask and 30 mL toluene was added into the mixture. After 30h stirring at room temperature, the pale reddish colored solution was filtered off and the volume was reduced to 5 mL and kept at 0°C. The colorless crystals suitable (very less amount) for X-ray analysis were obtained within 24h. Yield: 0.200 g (28%). ^{1}H NMR (400 MHz, $CDCl_3$, 298 K): δ 1.05 (*d*, *J*= 4.9 Hz, 24H, $CH(CH_3)_3$), 1.15 (*s*, 36H, C*Me*$_3$), 3.54-3.65 (*m*, 4H, $CH(CH_3)_3$), 7.05-7.07 (*m*, 2H, Ph), 7.18-7.19 (*m*, 3H, Ph), 7.37-7.56 (*m*, 24H, Ph), 7.65-7.76 (*m*, 4H, Ph), 8.57 (*bs*, 3H, Ph) ppm. $^{13}C\{^{1}H\}$ NMR (100.613 MHz, $CDCl_3$, 298 K): δ 22.65, 27.41, 29.77, 55.82, 122.53, 127.20, 127.25, 127.31, 127.38, 128.02, 128.61, 128.65, 130.78, 130.82, 130.86, 130.95 ppm. $^{31}P\{^{1}H\}$ NMR (161.97 MHz, $CDCl_3$, 298 K): δ 20.67. $^{19}F\{^{1}H\}$ NMR (376.49 MHz, $CDCl_3$, 298 K): δ -148.99 and -151.48 ppm. $^{11}B\{^{1}H\}$ NMR (128.387 MHz, $CDCl_3$, 298 K): δ -0.85 (*s*) and 0.94 (*br*). ^{119}Sn (149.18 MHz, $CDCl_3$, 298 K): δ -549.39 (*d*, *J*= 4638.8 Hz). HRMS: *m/z* [$C_{78}H_{100}N_8Sn_2P_2O_6B_4F_6$]: 1701.9847 [M-2H]$^+$. IR (cm^{-1}): 540.99, 587.68, 691.90, 791.57, 874.40, 1012.26, 1188.66, 1257.55, 1320.32, 1403.48, 1439.29, 1609.03, 2962.61, 3319.70.

Synthesis of 11:

25 mL toluene was added into the mixture of $GeCp^*_2$ (0.172 g, 0.5 mmol) and $NOBF_4$ (0.058 g, 0.5 mmol) in a 100 mL Schlenk flask. After overnight stirring, the reaction mixture was filtered off and the solvent was reduced to 5 mL. Colorless crystals of **11** suitable for X-ray analysis were obtained at 0°C.[S2]

Synthesis of 12:

30 mL toluene was added into the mixture of disilene $Cp^*SiN(TMS)_2{=}SiN(TMS)_2Cp^*$ (0.300 g, 0.464 mmol) and $NOBF_4$ (0.054 g, 0.464 mmol) in a 100 mL Schlenk flask. After overnight stirring, the reaction mixture was filtered off and the solvent was reduced to 5 mL. Colorless crystals suitable for X-ray analysis were obtained at 0°C. Yield: 0.145 g (46%). ^{1}H NMR (400 MHz, $CDCl_3$, 298K): δ 0.15- 0.28 (m, 36H, Si*Me*$_3$), 1.51- 2.06 (m, 30H, Cp*) ppm. $^{13}C\{^{1}H\}$ NMR (100.613 MHz, $CDCl_3$, 298 K): δ 2.83, 2.85, 3.15, 10.29, 10.39, 11.09, 20.41, 124.27, 127.20, 128.00, 136.79 ppm. $^{19}F\{^{1}H\}$ NMR (376.49 MHz, $CDCl_3$, 298): δ -125.43 and -133.70 ppm.

^{29}Si{^{1}H} NMR (79.495 MHz, CDCl$_3$, 298 K): δ 4.54, -15.36, -19.36 ppm. HRMS: *m/z* [$C_{32}H_{66}N_2Si_6F_2$]: 684.2068 [M]$^+$.

Synthesis of 13:

IPr and NOBF$_4$ (0.058 g, 0.5 mmol) were taken in 1:2 equivalent in a 100 mL Schlenk flask and 30 mL toluene was added into the mixture. After 24h stirring at room temperature, the pale yellow colored solution was filtered off and the volume was reduced to 5 mL and kept at 0^{o}C. The colorless crystals of **13** suitable for X-ray analysis were obtained within 24h.[S3]

S2. Crystal Data and Structure Refinements for 3-6, 8, 10 and **12:** All the crystal datas were collected on a Bruker Smart Apex Duo diffractometer at 100 K using Mo K$_\alpha$ radiation (λ = 0.71073 Å). The absorption correction was done using multi-scan method (SADABS). The structures were solved by direct methods and refined by full-matrix least-squares methods against F^2 (SHELXL-2014/6). Crystallographic data file (including structure factors) for the **3-6**, **8**, **10** and **12** have been deposited with the Cambridge Crystallographic Data Centre.

Table S1. Crystallographic details for **3-6, 8**, **10** and **12.**

	3	4	5	6
Chemical formula	$C_{21}H_{41}BF_3N_3OSi_3$	$C_{21}H_{41}BF_3GeN_3OSi_2$	$C_{21}H_{41}F_2N_3Si_3$	$C_{21}H_{41}F_2N_3GeSi_2$
Formula weight	503.65	548.15	457.84	502.34
Temperature	100(2)	100(2)	100(2)	100(2)
Wavelength	0.71073	0.71073	0.71073	0.71073
Crystal system	monoclinic	monoclinic	monoclinic	monoclinic
Space group	*Pn*	*Pn*	$P2_1/c$	*P*21/*c*
Unit cell dimentions	a=8.81(5) Å	a= 8.74(2) Å	a=18.681(7) Å	*a*= 18.850(11) Å
	b=17.21(10) Å	b= 17.01(4) Å	b=8.385(3) Å	*b*= 8.419(5) Å
	c=18.39(10) Å	c= 18.55(3) Å	c=18.595(7) Å	*c*= 18.595(11) Å
	α=90°	α=90°	α=90°	*α*=90°
	β=95.0(3)°	β= 95.21(9)°	β=116.752(9)°	*β*=117.495(11)°
	γ=90°	γ=90°	γ=90°	*γ*=90°
Volume	2778(27) Å^3	2748(11) Å^3	2600.9(17) Å^3	2618(3) Å^3
Z	4	4	4	4
Density (calculated)	1.204 g/cm^3	1.325 g/cm^3	1.169 g/cm^3	1.275 g/cm^3

Absorption coefficient	0.209 mm^{-1}	1.240 mm^{-1}	0.209 mm^{-1}	1.288 mm^{-1}
F(000)	1080	1152	992	1064
Theta range for data collection	2.22 to 25.00°	2.20 to 24.99°	2.19 to 24.99°	2.19 to 24.99°
Reflections collected	92850	71335	74158	75551
Independent reflections	9779 [R(int)= 0.2180]	9677 [R(int)= 0.2063]	4704 [R(int)= 0.0996]	4594 [R(int)= 0.3903]
Coverage of independent reflections	100%	99.9%	100%	100%
Data/ restraints/ parameters	9779/ 2/ 601	9677/ 2/ 601	4570/ 0/ 274	4594/ 0/ 274
Goodness-of-fit on F2	1.064	1.026	1.035	1.017
Δ/ σ max	0.000	0.001	0.000	0.000
Final R indices	6101 data; [I>2σ(I)] R1= 0.0688, wR2= 0.1298	6457 data; [I>2σ(I)] R1= 0.0675, wR2= 0.1184	3463 data; [I>2σ(I)] R1= 0.0407, wR2= 0.0822	2639 data; [I>2σ(I)] R1= 0.0662, wR2= 0.1073
	all data, R1= 0.1426, wR2= 0.1579	all data, R1= 0.1262, wR2= 0.1409	all data, R1= 0.0664, wR2= 0.0928	all data, R1= 1.017, wR2= 0.1339
Largest diff. peak and hole	0.441 and -0.512 $eÅ^{-3}$	0.910 and -0.914 $eÅ^{-3}$	0.273 and -0.273 $eÅ^{-3}$	0.497 and -0.709 $eÅ^{-3}$
R. M. S deviation from mean	0.083 $eÅ^{-3}$	0.110 $eÅ^{-3}$	0.050 $eÅ^{-3}$	0.107 $eÅ^{-3}$
Exposure time	15	15	20	20
Scan width	0.5	0.5	0.5	0.5

	8	**10**	**12**
Chemical formula	$C_{21}H_{41}F_2N_3SnSi_2$	$C_{99}H_{123}B_4F_6N_8O_6P_2Sn_2$	$C_{32}H_{66}F_2N_2Si_6$
Formula weight	548.44	1977.61	685.40
Temperature	100(2)	100(2)	100(2)
Wavelength	0.71073	0.71073	0.71073
Crystal system	monoclinic	monoclinic	triclinic

Space group	$P2_1/c$	$P2_1/n$	*P-1*
Unit cell dimentions	a= 18.489(8) Å	a= 17.1560(8) Å	a= 9.356(12) Å
	b= 8.832(4) Å	b= 17.9049(9) Å	b= 9.434(12) Å
	c= 18.866(8) Å	c= 17.4050(8) Å	c= 13.182(17) Å
	α= 90°	α= 90°	α= 95.79(3) °
	β=118.897(12)°	β= 112.890(2)	β= 106.56(3) °
	γ= 90°	γ= 90°	γ= 116.50(2) °
Volume	2697(2) Å^3	4925.4(4) Å^3	962(2) Å^3
Z	4	2	1
Density (calculated)	1.351 g/cm^3	1.333 g/cm^3	1.183 g/cm^3
Absorption coefficient	1.062 mm^{-1}	0.607 mm^{-1}	0.251 mm^{-1}
F(000)	1136	2050	374
Theta range for data collection	2.46 to 25.24°	2.13 to 25.24°	2.05 to 24.99°
Reflections collected	121073	87249	11819
Independent reflections	7435 [R(int)= 0.1079]	10098 [R(int)= 0.0894]	3369 [R(int)= 0.2677]
Coverage of independent reflections	100%	99.9%	99.6%
Data/ restraints/ parameters	7435/ 0/ 274	10098 / 0/ 610	3369 / 0/ 201
Goodness-of-fit on F2	1.033	1.157	1.019
Δ/ σ max	0.000	0.001	0.000
Final R indices	4757 data; [I>2σ(I)] R1= 0.0529, wR2= 0.1080	7158 data; [I>2σ(I)] R1= 0.0659, wR2= 0.1615	1402 data; [I>2σ(I)] R1= 0.1075, wR2= 0.1847
	all data, R1= 0.1109, wR2= 0.1276	all data, R1= 0.1102, wR2= 0.2126	all data, R1= 0.2559, wR2= 0.2380
Largest diff. peak and hole	1.480 and -0.953 eÅ^{-3}	2.991 and -1.102 eÅ^{-3}	0.510 and -0.443 eÅ^{-3}
R. M. S deviation from mean	0.111 eÅ^{-3}	0.153 eÅ^{-3}	0.095 eÅ^{-3}
Exposure time	30	20	25
Scan width	0.5	0.5	0.5

S3. Computational Methodology

All the geometries were optimized at the DFT level of theory BP86[S4] comprising the exchange functional of Becke in conjunction with the correlation functional of Perdew using Gaussian 09 program package. [S5] The basis set def2-SVP[S6], a double ζ-quality augmented with one set of polarization functions, is used for the geometry optimization. The single point calculations were performed using meta-GGA exchange correlation functional M06[S7] with basis set having triple ζ-quality augmented by two sets of polarization functions (def2-TZVPP).[S8] The Natural Bond Orbital analysis (NBO)[S9] was performed at the M06/def2-TZVPP//BP86/def2-SVP level of theory which gives best Lewis representation of the compound along with atomic and bond descriptors like natural charge, bond type, bond order, second order donor-acceptor interactions etc. The quantitative analysis of Molecular electrostatic potential (MESP)[S9] on the molecular van der Waals surfaces using Multiwfn[S10] program was carried out at the M06/def2-TZVPP//BP86/def2-SVP level of theory. The MESP analysis has been used for the prediction of nucleophilic and electrophilic sites, the strength and orientation of weak interaction such as hydrogen bonding, dihydrogen bonding and halogen bonding. by analyzing the magnitude and positions of minima and maxima of the potential energy on the van der Waals surface. Energy Decomposition Analysis (EDA)[S11] of **3′**, **4′**, **3** and **4** was carried out at the BP86/TZ2P level of theory with a frozen-core approximation for the core electrons using ADF 2016.01 program.[S12] EDA is a fragment based method for understanding the nature of a chemical bond. It focuses on the instantaneous interaction energy (ΔE_{int}) of a bond between two fragments in the frozen geometry of the compound. ΔE_{int} is divided into three chemically meaningful terms: Electrostatic interaction (ΔE_{elstat}), Pauli's repulsion (ΔE_{Pauli}) and Orbital interactions (ΔE_{orb}).

$$\Delta E_{int} = \Delta E_{elstat} + \Delta E_{Pauli} + \Delta E_{orb}$$

ΔE_{elstat} gives the quasi classical electrostatic interaction energy between the frozen charge densities of the fragments and in most cases it is stabilizing attractive interaction. ΔE_{Pauli} represents the destabilizing repulsive interactions between the electrons of the same spin in the two fragments. ΔE_{orb} is the energy lowering comes from the orbital mixing when the two fragments are allowed to overlap and is always attractive. The electronic state of the fragments which leads to lowest ΔE_{orb} is considered as the best bonding description. EDA-NOCV (Energy Decomposition Analysis

– Natural Orbital for Chemical Valence) analysis[S13] is an extension of EDA analysis which combines charge with energy partitioning scheme. In EDA-NOCV scheme, ΔE_{orb} term is decomposed into pairwise contributions from different Natural Orbitals of Chemical Valence (NOCV)[9] and associated deformation densities ($\Delta\rho$) which is the difference between the charge densities of fragments before and after bond formation. The NOCVs (φ_i) are defined as the Eigen vectors of the chemical valence operator ($\hat{V}$) of the Nalewajski-Mrozek theory of valence and bond order indices and is given by

$$\hat{V}\varphi_i = \vartheta_i\varphi_i \qquad i = 1 - \mathrm{N}$$

In the molecular systems with multiple bonds, NOCV can be grouped in pairs of complementary orbitals (φ_{-i}, φ_i) corresponding to the same eigenvalue (ϑ_i) with the opposite sign. The deformation density ($\Delta\rho$) can be expressed as the sum of the complementary pairs of NOCV.

$$\Delta\rho = \sum_{i=1}^{N/2} \Delta\rho_i = \sum_{i=1}^{N/2} v_i \left[-\varphi_{-i}^{2} + \varphi_i^2 \right]$$

The plot of deformation density helps to determine the direction of charge flow after the bond formation. Figure S5 and S6 shows the deformation density plot of **3′**, **4′**, **3** and **4** respectively. The direction of charge flow is from red to blue.

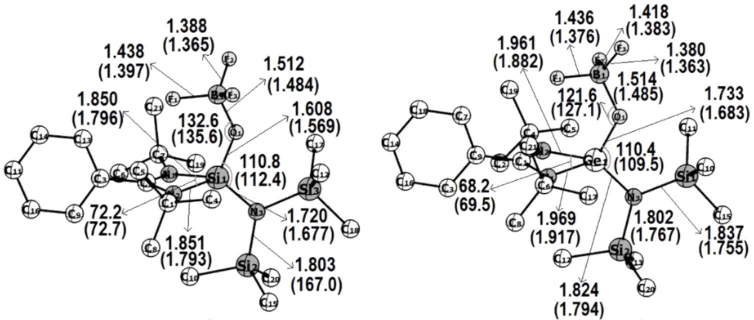

3

4

(a)

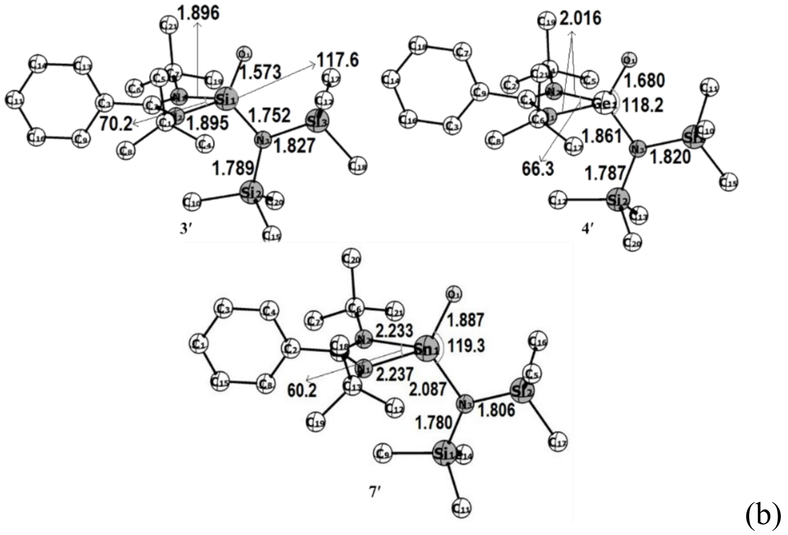

Figure S1. Optimized geometries and important geometrical parameters of **a**). BF_3 coordinated sila- and germa acetamide **3** and **4** and **b**). sila- and gema-acetamide without BF_3 **3′** and **4′**. Distances are given in A° and angles are in (°). Hydrogens are omitted for clarity.

Table S2. Natural charge and Wiberg Bond Index (**WBI**) of **3, 4, 3′** and **4′** given by the natural population analysis calculated at the M06/def2-TZVPP//BP86/def2-SVP level of theory.

		Charge		**WBI**
	Si1	**O**	**B**	**Si1−O**
3	2.45	-1.17	1.34	0.70
3′	2.32	-1.29	-	1.07
	Ge	**O**	**B**	**Ge−O**
4	2.32	-1.13	1.33	0.70
4′	2.19	-1.23	-	1.09

Table S3. Second order perturbation interactions and bond occupancy of the selected bonds in **3**, **4**, **3′** and **4′** given by the natural population analysis calculated at the M06/def2-TZVPP//BP86/def2-SVP level of theory.

	3			**4**	
Donor	**Acceptor**	**Energy (kcal/mol)**	**Donor**	**Acceptor**	**Energy (kcal/mol)**
LP(2) O	BD*(1) Si-N1	10.7	LP(1) O	BD*(1) Ge1-N1	6.37
LP(2) O	BD*(1) Si-N2	7.00	LP(2)O	BD*(1) Ge1-N1	4.26
LP(2) O	BD*(1) F2-B14	7.01	LP(2) O	BD*(1) F2-B	7.68
LP(1) O	BD*(1) Si-N1	2.50	LP(2) O	BD*(1) Ge1-N2	10.47
LP(1) O	BD*(1) Si-N2	5.74	LP(1) O	BD*(1) Ge1-N2	1.14
LP(1) O	BD*(1) F1-B	5.38	LP(1) O	BD*(1) F1-B	3.00

	3′			**4′**	
Donor	**Acceptor**	**Energy (kcal/mol)**	**Donor**	**Acceptor**	**Energy (kcal/mol)**
BD (2) Si1–O	BD*(1) Si1–N2	20.6	BD (2)Ge1–O	BD*(1)Ge1–N2	30.2
BD (2) Si1–O	BD*(1) Si1–N1	18.0	BD (2)Ge1–O	BD*(1)Ge1–N1	14.7
BD (3) Si1–O	BD*(1) Si1–N3	16.7	BD (3)Ge1–O	BD*(1)Ge1–N3	15.2
LP (1) O1	RY (1) Si1	10.9	LP (1) O4	RY (1)Ge1	6.9

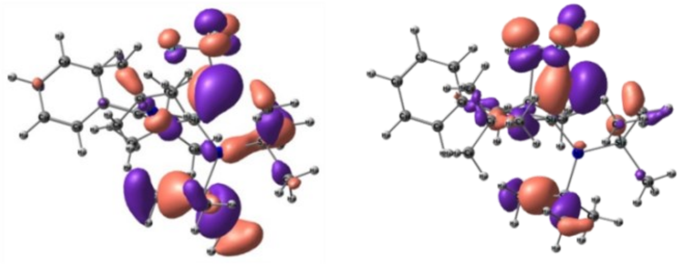

HOMO-7 (-8.69) HOMO-8 (-8.83)

3

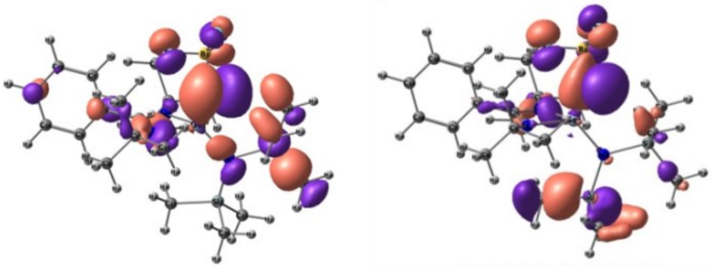

HOMO-4 (-8.30) HOMO-8 (-8.76)

4

Figure S2. Plots of molecular orbitals representing the lone pair on oxygen atom in **3** and **4**. Isosurface value is 0.03. Energies are given in eV

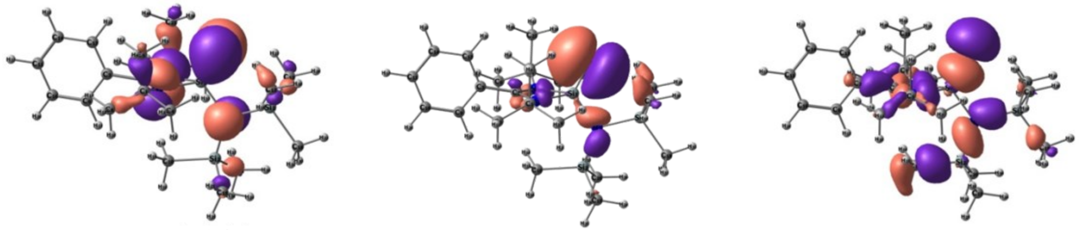

HOMO (-6.46) **HOMO-1 (-6.62)** **HOMO-9 (-8.30)**

3′

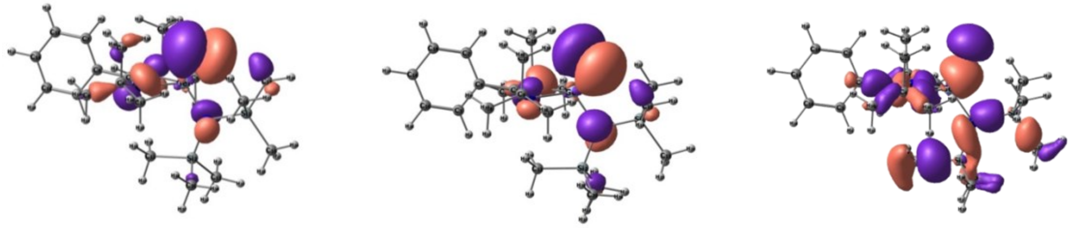

HOMO (-6.41) **HOMO-1 (-6.44)** **HOMO-9 (-8.29)**

4′

Figure S3. Plots of molecular orbitals representing the lone pair on oxygen atom in **3′** and **4′**. Isosurface value is 0.03. Energies are given in eV.

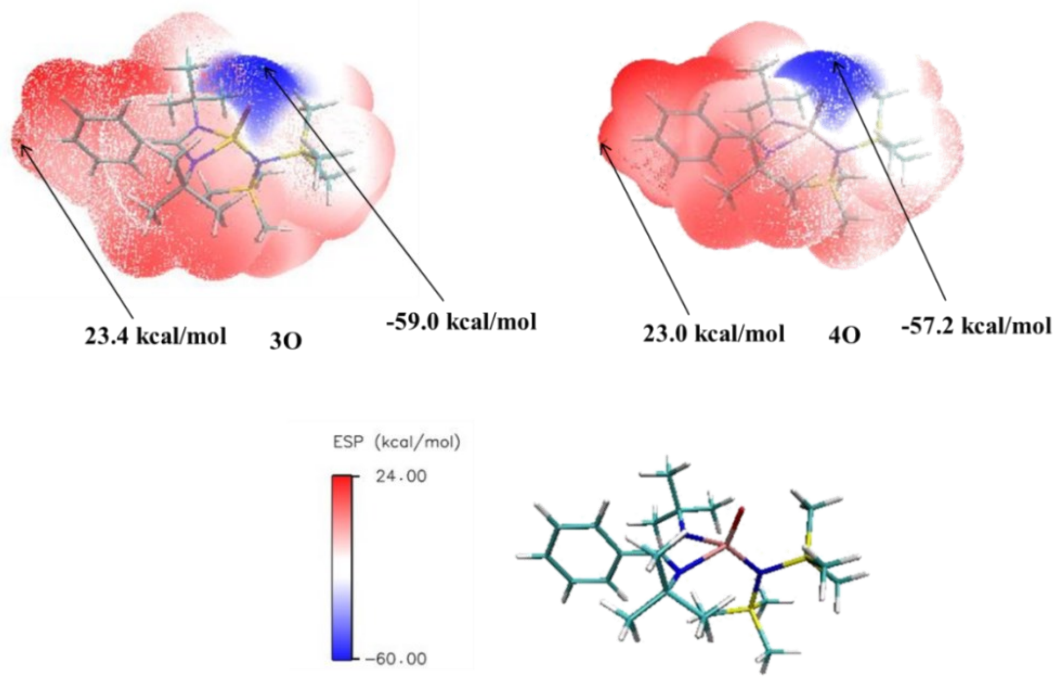

Figure S4. Plot of molecular electrostatic potential (kcal/mol) on the molecular van der Waals surfaces of **3′** and **4′** at the M06/def2-TZVPP//BP86/def2-SVP level of theory. The global minima and global maxima are given in italics

Table S4. Molecular electrostatic potential values on the local molecular surface of oxygen atom in **3′**, **4′**, **3** and **4** calculated at the M06/def2-TZVPP//BP86/def2-SVP level of theory.

	ESP (kcal/mol)		**ESP (kcal/mol)**
3′	-52.9	**4′**	-51.7
3	-32.9	**4**	-35.3

Table S5. Reaction energy for the formation of **3** and **4** from the reaction of **3′** and **4′** with BF_3 and the reaction energy for the formation of hypothetical compounds **3′**, **4′** and **7′** calculated at the M06/def2-TZVPP//BP86/def2-SVP level of theory

Reaction			**Reaction Energy (kcal/mol)**
3′ + BF_3	$\longrightarrow$	**3**	-40.3
4′ + BF_3	$\longrightarrow$	**4**	-40.8
1 + O	$\longrightarrow$	**3′**	-149.6
2 + O	$\longrightarrow$	**4′**	-99.5
7 + O	$\longrightarrow$	**7′**	-68.5

The quantitative analysis of Molecular Electrostatic Potential (MESP) on the molecular van der Waals surfaces of the compounds **3′**, **4′**, **3** and **4** were performed to understand the nucleophilicity of the oxygen atom. The MESP analysis of **3′** and **4′** show a global minimum (-59.0 kcal/mol and -57.2 kcal/mol) in the direction of lone pair of oxygen atom, indicating its high nucleophilicity (Figure S4). The MESP values on the van der Waals surface of oxygen atom in **3′** and **4′** are -52.9 kcal/mol and -51.7 kcal/mol respectively, whereas it is decreased to -32.9 kcal/mol and -35.3 kcal/mol in **3** and **4** respectively (Table S4)**.** This indicates that the reactivity of oxygen atom in **3′** and **4′** is getting reduced on coordination with the Lewis acid BF_3 and hence, stabilizes the sila- and germa- acetamide **3′** and **4′**. This is well supported by high exothermic reaction energy for the formation of BF_3 adduct from **3′** (-40.3 kcal/mol) and **4′** (-40.8 kcal/mol, Table S5). The high BF_3 binding energy of **3′** and **4′** is attributed to the multiply bonded Si–O and Ge–O resulting from the hyperconjugative interaction of the oxygen lone pairs.

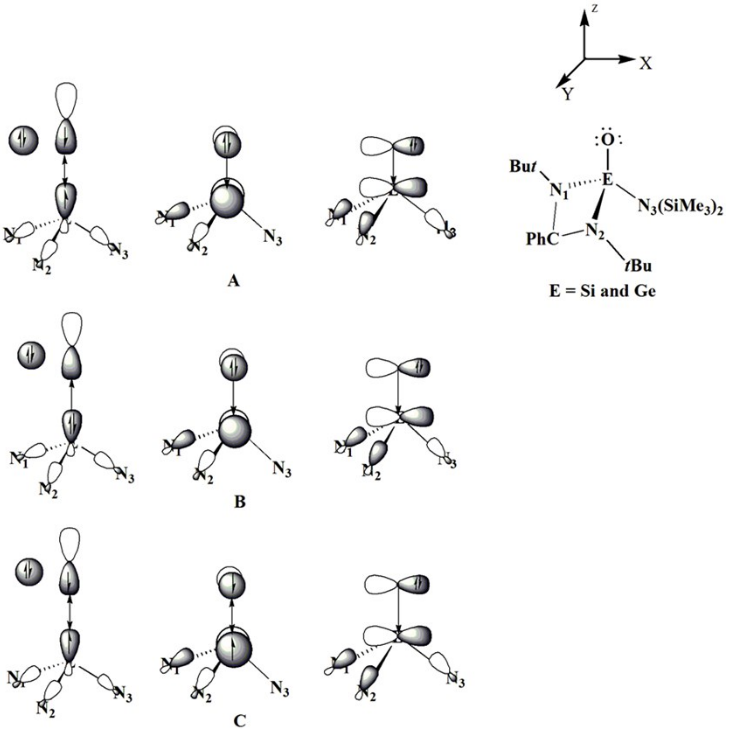

Scheme S1. Schematic representation of different bonding possibilities for the interaction between the group orbitals on PhC(N*t*Bu)$_2$EN(SiMe$_3$)$_2$ and the oxygen atom in **3′** and **4′** used for the EDA-NOCV analysis. Scheme **A** represents the bonding interaction between the charged fragments [PhC(N*t*Bu)$_2$EN(SiMe$_3$)$_2$]$^{+1}$ and O^{-1} and **B** and **C** represents the bonding interaction between the neutral fragments. Double headed arrow (↔) indicates the electron sharing interaction and the single headed arrow (→) indicates the donor-acceptor interaction between the fragments.

Table S6. EDA-NOCV data of all the bonding possibilities of **3′**, **4′**, **3** and **4** calculated at the BP86/TZ2P level of theory. Energies are given in kcal/mol.

		ΔE_{int}	**ΔE_{Pauli}**	**ΔE_{Elstat}**	**ΔE_{Orb}**
3′	**A**	-264.7	337.6	-309.2	-293.2
	B	-225.2	417.9	-170.7	-472.4
	C	-241.7	309.3	-150.5	-400.5
4′	A	-232.0	285.9	-280.1	-237.8
	B	-181.6	313.2	-128.1	-366.7
	C	-203.4	253.9	-128.5	-328.8
3	**A**	-204.6	393.0	-292.9	-304.7

	B	-234.9	539.4	-264.8	-509.6
	C	-278.8	385.9	-185.1	-479.5
4	**A**	-176.0	-249.5	305.5	-232.1
	B	-196.5	-197.8	406.9	-405.6
	C	-244.3	-158.8	317.7	-403.2

Table S7. EDA-NOCV results of the best possible bonding representation (**A** in Scheme S1) of **3′**, **4′**, **3** and **4** calculated at the BP86/TZ2P level of theory. Energies are given in kcal/mol.

	ΔE_{int}	ΔE_{Pauli}	ΔE_{Elstat}	ΔE_{Orb}	$^{a}\Delta E_1$	$^{b}\Delta E_2$	$^{b}\Delta E_3$	$^{b,c}\Delta E_{rest}$	ΔE_{prep}	$-D_e$
3′	-264.7	337.6	-309.2 (51.3%)	-293.2 (48.6%)	-196.9 (67.1%)	-35.3 (12.0%)	-32.4 (11.0%)	-28.6 (9.7%)	101	-163.7
4′	-232.0	285.9	-280.1 (54.1%)	-237.8 (45.9%)	-161.9 (68.1%)	-28.7 (12.1%)	-23.2 (9.7%)	-24.0 (10.1%)	114.6	-117.4
3	-204.6	393.0	-292.9 (49.0%)	-304.7 (50.9%)	-237.4 (77.9%)	-22.7 (7.4%)	-21.1 (6.9%)	-23.5 (7.7%)	9.0	-195.6
4	-176.0	305.5	-249.5 (51.8%)	-232.1 (48.1%)	-181.2 (78.0%)	-15.9 (6.8%)	-12.8 (5.5%)	-22.2 (9.5%)	8.8	-167.2

[a] Values in parenthesis give the percentage contribution to the total attractive interaction $\Delta E_{Elsta} + \Delta E_{Orb}$. [b] Values in parenthesis give the percentage contribution to the total orbital interaction ΔE_{Orb}. [c] $\Delta E_{rest} = \Delta E_{Orb} - (\Delta E_1 + \Delta E_2 + \Delta E_3)$.

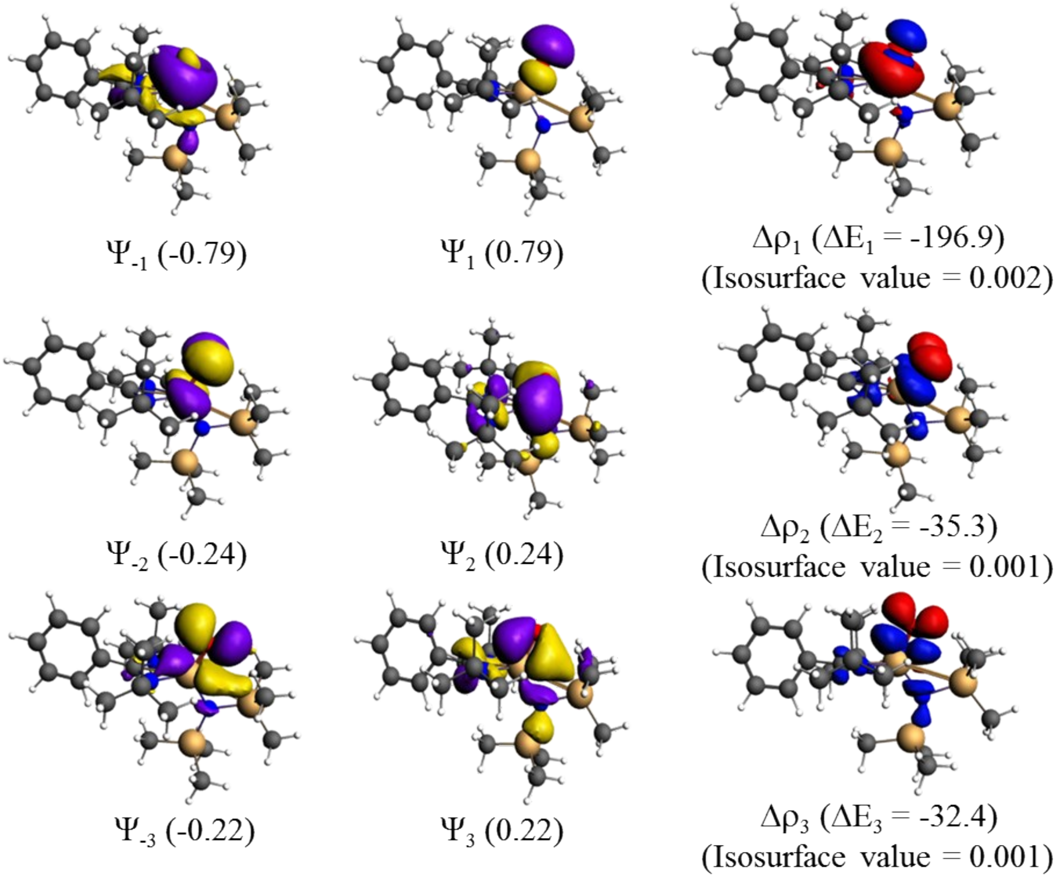

Ψ_{-1} (-0.79)

Ψ_{1} (0.79)

$\Delta\rho_1$ (ΔE_1 = -196.9)
(Isosurface value = 0.002)

Ψ_{-2} (-0.24)

Ψ_{2} (0.24)

$\Delta\rho_2$ (ΔE_2 = -35.3)
(Isosurface value = 0.001)

Ψ_{-3} (-0.22)

Ψ_{3} (0.22)

$\Delta\rho_3$ (ΔE_3 = -32.4)
(Isosurface value = 0.001)

Figure S5. Plots of α-NOCV pair of orbitals $\psi_{-n}, \psi_n$with their eigen values in the parenthesis, the associated deformation densities $\Delta\rho_n$and the associated orbital stabilization energies ΔE of **3′** (in kcal/mol) at the BP86/TZ2P level of theory. The isosurface value for the NOCV plots is 0.03 and for the deformation densities is given in the paranthesis.

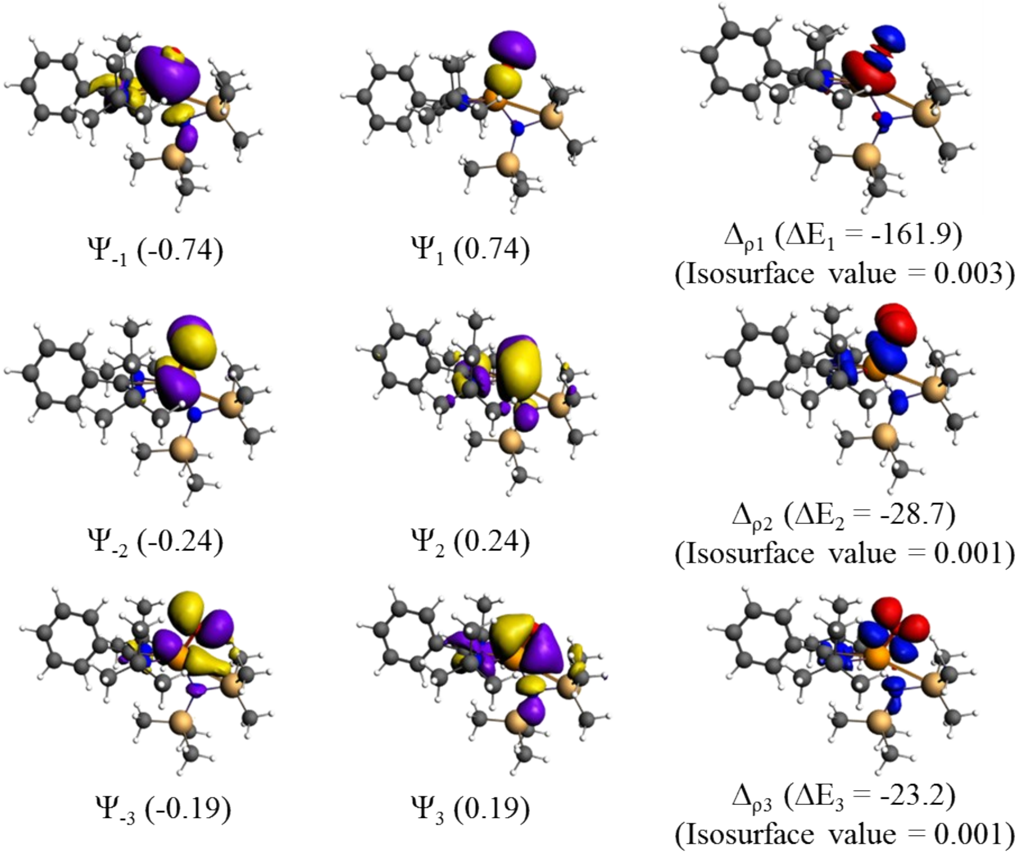

Ψ_{-1} (-0.74)

Ψ_{1} (0.74)

$\Delta_{\rho 1}$ ($\Delta E_1 = -161.9$)
(Isosurface value = 0.003)

Ψ_{-2} (-0.24)

Ψ_{2} (0.24)

$\Delta_{\rho 2}$ ($\Delta E_2 = -28.7$)
(Isosurface value = 0.001)

Ψ_{-3} (-0.19)

Ψ_{3} (0.19)

$\Delta_{\rho 3}$ ($\Delta E_3 = -23.2$)
(Isosurface value = 0.001)

Figure S6. Plots of α-NOCV pair of orbitals ψ_{-n}, ψ_n with their eigen values in the parenthesis, the associated deformation densities $\Delta\rho_n$ and the associated orbital stabilization energies ΔE of **4′** (in kcal/mol) at the BP86/TZ2P level of theory. The isosurface value for the NOCV plots is 0.03 and for the deformation densities is given in the paranthesis.

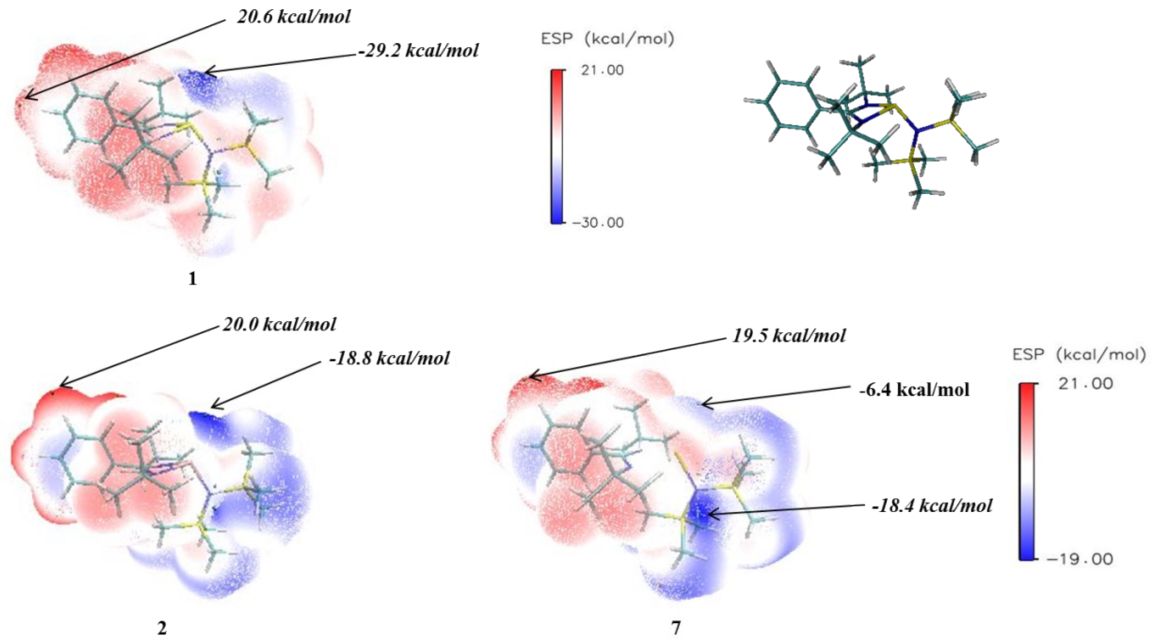

Figure S7. Plot of electrostatic potential (kcal/mol) on the molecular van der Waals surfaces of **1**, **2** and **7** at the M06/def2-TZVPP//BP86/def2-SVP level of theory. The global minima and global maxima are given in italics.

Table S8. Optimized Cartesian coordinates and total energies (in a.u.) including zero point energy correction of all the calculated molecules at the BP86/def2-SVP level of theory (E1) and total energy at M06/def2-TZVPP level of theory including zero point energy correction from the BP86/def2-SVP level of theory (E2) using G09 program package.

3

E1 = -2255.886449

E2 = -2256.825318

14	-0.625497000	0.292933000	0.073668000
14	-2.289234000	-2.310013000	-0.160548000
14	-3.599173000	0.601426000	0.097250000
9	1.440730000	2.585697000	0.039329000
8	-0.836178000	1.878134000	0.244622000
9	-0.113805000	3.942580000	1.095540000
9	-0.215618000	3.623095000	-1.207032000
7	0.772183000	-0.335957000	1.109158000
7	0.759126000	-0.167891000	-1.065123000
7	-2.138982000	-0.522745000	0.024485000
6	1.054593000	0.040547000	-2.514473000
6	1.559043000	-0.376985000	0.007972000
6	3.035239000	-0.582990000	-0.014483000
5	0.083664000	3.061360000	0.041853000
6	-0.203807000	0.715672000	-3.100042000
1	-0.351173000	1.720712000	-2.653320000
1	-1.109543000	0.101004000	-2.914853000
1	-0.092828000	0.834699000	-4.196505000
6	2.263531000	0.975649000	-2.732203000
1	3.222281000	0.489518000	-2.467585000
1	2.146358000	1.898516000	-2.131426000
1	2.315100000	1.253093000	-3.805070000
6	2.099078000	-1.378514000	2.962744000
1	3.104650000	-1.174934000	2.547896000
1	1.776312000	-2.385222000	2.624977000
1	2.192221000	-1.403443000	4.067786000
6	1.073275000	-0.296624000	2.567216000
6	1.293111000	-1.325059000	-3.194840000
1	0.406875000	-1.985426000	-3.096110000
1	2.171117000	-1.844323000	-2.759338000
1	1.490373000	-1.179483000	-4.277028000
6	3.574979000	-1.867230000	-0.241438000
1	2.904182000	-2.726852000	-0.394505000
6	-0.588086000	-3.149805000	-0.079629000

1	-0.089866000	-3.013247000	0.901005000
1	0.099401000	-2.796010000	-0.873390000
1	-0.742862000	-4.239791000	-0.230204000
6	5.823009000	-0.950067000	0.039769000
1	6.915061000	-1.093440000	-0.049047000
6	-3.599446000	1.764910000	-1.391186000
1	-3.621277000	1.200355000	-2.347259000
1	-2.709816000	2.425522000	-1.383942000
1	-4.506499000	2.406423000	-1.359740000
6	3.891466000	0.521915000	0.193751000
1	3.448557000	1.520104000	0.333287000
6	5.282521000	0.330070000	0.179949000
1	5.949393000	1.192331000	0.336962000
6	-3.036415000	-2.744571000	-1.848522000
1	-2.399601000	-2.367661000	-2.676366000
1	-4.052671000	-2.325421000	-1.989750000
1	-3.112609000	-3.847813000	-1.957929000
6	4.968760000	-2.046472000	-0.251691000
1	5.388048000	-3.050046000	-0.424787000
6	-3.614467000	1.552985000	1.730060000
1	-2.748291000	2.240345000	1.795584000
1	-3.600438000	0.863948000	2.601036000
1	-4.544280000	2.157959000	1.798334000
6	-5.216965000	-0.396125000	0.035212000
1	-5.407723000	-0.978465000	0.958961000
1	-5.312702000	-1.074747000	-0.835961000
1	-6.034049000	0.353316000	-0.048775000
6	-0.266191000	-0.581419000	3.279911000
1	-0.659491000	-1.584689000	3.017316000
1	-1.029700000	0.177548000	3.011667000
1	-0.124955000	-0.541408000	4.378526000
6	-3.319821000	-3.072778000	1.235903000
1	-4.398866000	-2.835169000	1.164537000
1	-2.959939000	-2.736646000	2.230878000
1	-3.219348000	-4.178952000	1.198086000
6	1.576041000	1.108613000	2.970441000
1	0.857483000	1.896316000	2.670482000
1	2.548053000	1.338862000	2.493831000
1	1.714074000	1.153370000	4.070854000

4

E1 = -4043.410214

E2 = -4044.215997

32	-0.625885000	0.297163000	-0.162914000
14	-3.679923000	0.566688000	-0.092445000
14	-2.344345000	-2.314421000	0.384012000
9	1.429185000	2.559655000	-0.641293000
8	-0.872943000	1.902162000	-0.768333000
9	-0.078070000	3.364838000	0.924774000
7	0.907879000	-0.561063000	-1.050182000
7	0.880904000	0.047478000	1.067462000
7	-2.226089000	-0.542012000	0.083248000
9	-0.197887000	4.088549000	-1.279418000
6	1.664645000	-0.377180000	0.054905000
6	1.664287000	-0.864626000	3.247995000
1	0.930512000	-1.695770000	3.196567000
1	1.821431000	-0.616169000	4.317769000
1	2.631558000	-1.221834000	2.841211000
6	3.692987000	-1.855263000	0.360624000
1	3.028315000	-2.722571000	0.496389000
6	1.152357000	0.382359000	2.494887000
6	-0.204047000	0.832929000	3.075651000
1	-0.547104000	1.749323000	2.553328000
1	-0.095692000	1.068881000	4.153115000
1	-0.972343000	0.038332000	2.973532000
6	1.263683000	-0.725176000	-2.489946000
6	3.993929000	0.540077000	-0.043661000
1	3.546160000	1.528904000	-0.228582000
6	1.893852000	-2.113225000	-2.734951000
1	2.852510000	-2.227850000	-2.191707000
1	2.102883000	-2.242044000	-3.816998000
1	1.209400000	-2.928087000	-2.420243000
6	3.143479000	-0.575727000	0.129800000
5	0.085938000	3.028228000	-0.442913000
6	-3.818423000	1.152140000	-1.882604000
1	-2.939213000	1.773647000	-2.145821000
1	-4.731813000	1.771095000	-2.013817000
1	-3.881852000	0.297343000	-2.588355000
6	-3.545611000	2.014908000	1.112359000
1	-3.549188000	1.663564000	2.165812000
1	-4.421889000	2.685473000	0.979120000
1	-2.629027000	2.613405000	0.938780000
6	-0.622298000	-3.091520000	0.544755000
1	-0.002365000	-2.966126000	-0.365058000
1	-0.755954000	-4.181096000	0.716513000
1	-0.056091000	-2.685402000	1.407587000
6	-3.245433000	-2.678789000	2.011571000
1	-2.782815000	-2.120864000	2.852852000
1	-3.163363000	-3.763060000	2.241348000
1	-4.322687000	-2.424214000	1.984918000
6	5.935042000	-0.908702000	0.247564000
1	7.027852000	-1.038659000	0.293557000
6	-5.271168000	-0.372992000	0.349269000
1	-5.442223000	-1.298512000	-0.236056000
1	-6.112562000	0.316532000	0.119310000
1	-5.338452000	-0.618688000	1.428253000
6	5.087839000	-2.016883000	0.422438000
1	5.513350000	-3.015770000	0.607176000
6	-0.073780000	-0.623737000	-3.254365000

1	-0.794664000	-1.391823000	-2.904186000
1	0.092772000	-0.780475000	-4.338771000
1	-0.528015000	0.379658000	-3.119811000
6	5.386492000	0.365199000	0.013355000
1	6.047491000	1.234971000	-0.126041000
6	2.155886000	1.551003000	2.617538000
1	3.175930000	1.250875000	2.309465000
1	2.207950000	1.875977000	3.677259000
1	1.820403000	2.406489000	2.000123000
6	-3.212848000	-3.169262000	-1.069818000
1	-4.247869000	-2.806510000	-1.232062000
1	-3.266771000	-4.264754000	-0.890957000
1	-2.649395000	-3.009389000	-2.013250000
6	2.207414000	0.400346000	-2.970541000
1	1.835364000	1.387730000	-2.633702000
1	2.267195000	0.389578000	-4.078377000
1	3.234591000	0.265001000	-2.578887000

3′

E1 = -1931.536161

E2 = -1932.174952

14	-0.656159000	0.018257000	-0.861066000
14	-2.090022000	0.044591000	1.961830000
14	-3.594154000	-0.035278000	-0.829844000
8	-0.892378000	0.071223000	-2.414953000
7	0.781638000	1.093046000	-0.250018000
7	0.774236000	-1.085822000	-0.291384000
7	-2.068382000	-0.022784000	0.174174000
6	1.073569000	-2.525755000	-0.476827000
6	1.563602000	-0.003722000	-0.132647000
6	3.035253000	-0.013148000	0.135660000
6	-0.267374000	-3.268357000	-0.293229000
1	-1.019340000	-2.915792000	-1.028098000
1	-0.675761000	-3.109790000	0.725396000
1	-0.124390000	-4.357319000	-0.445600000
6	1.582401000	-2.745651000	-1.922710000
1	2.586231000	-2.295610000	-2.063301000
1	0.883359000	-2.275315000	-2.644157000
1	1.662146000	-3.829580000	-2.148329000
6	2.178637000	3.079915000	0.420215000
1	3.169176000	2.606648000	0.279244000
1	1.875335000	2.950448000	1.479923000
1	2.297552000	4.166819000	0.230994000
6	1.112844000	2.512076000	-0.538820000
6	2.091069000	-3.058756000	0.552484000
1	1.748362000	-2.866212000	1.590269000
1	3.094711000	-2.609429000	0.427277000
1	2.196854000	-4.156205000	0.427450000
6	3.502243000	0.033848000	1.468007000
1	2.778004000	0.075775000	2.295911000
6	-0.337653000	0.015499000	2.694633000
1	0.272721000	0.873278000	2.348965000
1	0.201585000	-0.920764000	2.446318000
1	-0.424664000	0.076950000	3.800547000
6	5.805270000	-0.031008000	0.673967000
1	6.886464000	-0.038064000	0.883897000
6	-3.626906000	-1.523025000	-2.000017000
1	-3.562847000	-2.481588000	-1.442188000
1	-2.770626000	-1.445168000	-2.699986000
1	-4.573055000	-1.533158000	-2.583241000
6	3.965698000	-0.068352000	-0.925416000
1	3.607983000	-0.102157000	-1.965960000
6	5.344781000	-0.075661000	-0.653490000
1	6.063363000	-0.116482000	-1.487197000
6	-2.983963000	-1.448071000	2.726430000
1	-2.566382000	-2.403009000	2.343002000
1	-4.074093000	-1.452278000	2.531182000
1	-2.841751000	-1.437979000	3.828887000
6	4.881029000	0.023096000	1.732844000
1	5.235603000	0.057858000	2.775055000
6	-3.746096000	1.578853000	-1.807690000
1	-2.887973000	1.644639000	-2.507250000
1	-3.745168000	2.467673000	-1.141808000
1	-4.688208000	1.594372000	-2.396898000
6	-5.142324000	-0.192907000	0.269608000
1	-5.243618000	0.587821000	1.050135000
1	-5.223015000	-1.186401000	0.755726000
1	-6.018798000	-0.090667000	-0.407074000
6	-0.202818000	3.298017000	-0.355487000
1	-0.571417000	3.221719000	0.687805000
1	-0.990402000	2.911630000	-1.034202000
1	-0.044583000	4.370190000	-0.589665000
6	-2.893191000	1.654505000	2.574559000
1	-3.935054000	1.780941000	2.217380000
1	-2.313660000	2.536802000	2.230047000
1	-2.914675000	1.677318000	3.685518000
6	1.574893000	2.627274000	-2.012018000
1	0.834398000	2.135428000	-2.676150000
1	2.558740000	2.135447000	-2.156896000
1	1.682377000	3.692359000	-2.305913000

4′

E1 = -3719.058550

E2 = -3719.564787

32	0.661943000	0.071704000	-0.852674000
14	3.679449000	-0.017192000	-0.724124000
14	2.110791000	-0.042521000	2.044967000
8	0.916723000	0.248708000	-2.503708000
7	-0.912380000	1.112039000	-0.144267000
7	-0.898424000	-1.085203000	-0.313517000
7	2.148494000	-0.058168000	0.258670000
6	-1.669961000	-0.004570000	-0.101216000

6	-2.165869000	-3.074856000	0.569190000
1	-1.777327000	-2.886929000	1.591458000
1	-2.267822000	-4.172286000	0.440201000
1	-3.177914000	-2.633287000	0.494200000
6	-3.591366000	-0.017946000	1.520335000
1	-2.856257000	0.007888000	2.339440000
6	-1.200976000	-2.522036000	-0.501553000
6	0.151916000	-3.258884000	-0.388990000
1	0.866187000	-2.894036000	-1.155642000
1	0.010200000	-4.347425000	-0.545400000
1	0.608840000	-3.106646000	0.609729000
6	-1.264544000	2.532258000	-0.396503000
6	-4.085058000	-0.065197000	-0.868067000
1	-3.741132000	-0.070541000	-1.913858000
6	-2.351137000	3.057632000	0.565086000
1	-3.333102000	2.576358000	0.395680000
1	-2.481123000	4.148466000	0.407815000
1	-2.060696000	2.898165000	1.624184000
6	-3.140874000	-0.031699000	0.181475000
6	3.832410000	1.659818000	-1.588493000
1	2.976769000	1.765461000	-2.288085000
1	4.775615000	1.725709000	-2.172290000
1	3.816689000	2.500687000	-0.863291000
6	3.678365000	-1.407624000	-2.007550000
1	3.578617000	-2.406363000	-1.531817000
1	4.625858000	-1.398870000	-2.588421000
1	2.829775000	-1.243965000	-2.703951000
6	0.336803000	-0.092996000	2.718095000
1	-0.266734000	0.770457000	2.374306000
1	0.387220000	-0.061697000	3.827533000
1	-0.190573000	-1.024034000	2.427047000
6	2.982923000	-1.559760000	2.787401000
1	2.563519000	-2.501257000	2.373634000
1	2.823224000	-1.575701000	3.887500000
1	4.076138000	-1.568519000	2.609286000
6	-5.904252000	-0.073250000	0.755012000
1	-6.982606000	-0.089101000	0.978636000
6	5.204075000	-0.276105000	0.384145000
1	5.298792000	0.449509000	1.217187000
1	6.098231000	-0.147327000	-0.264038000
1	5.251030000	-1.301119000	0.805042000
6	-4.966349000	-0.041522000	1.802921000
1	-5.307623000	-0.033340000	2.850142000
6	0.035649000	3.333936000	-0.169776000
1	0.392596000	3.227762000	0.875118000
1	-0.137154000	4.410815000	-0.369257000
1	0.838022000	2.986133000	-0.852952000
6	-5.460746000	-0.083576000	-0.578851000
1	-6.189920000	-0.105797000	-1.404042000
6	-1.776396000	-2.736709000	-1.922590000
1	-2.780363000	-2.276446000	-2.019056000
1	-1.876830000	-3.820025000	-2.142924000
1	-1.106274000	-2.278875000	-2.678595000
6	2.904069000	1.545869000	2.725280000
1	3.960264000	1.667753000	2.409891000
1	2.884381000	1.545064000	3.836567000
1	2.347496000	2.441731000	2.377441000
6	-1.708169000	2.687089000	-1.871756000
1	-0.947515000	2.236612000	-2.543246000
1	-1.836492000	3.758723000	-2.131971000
1	-2.678228000	2.178174000	-2.047545000

S4. Molecular Structure

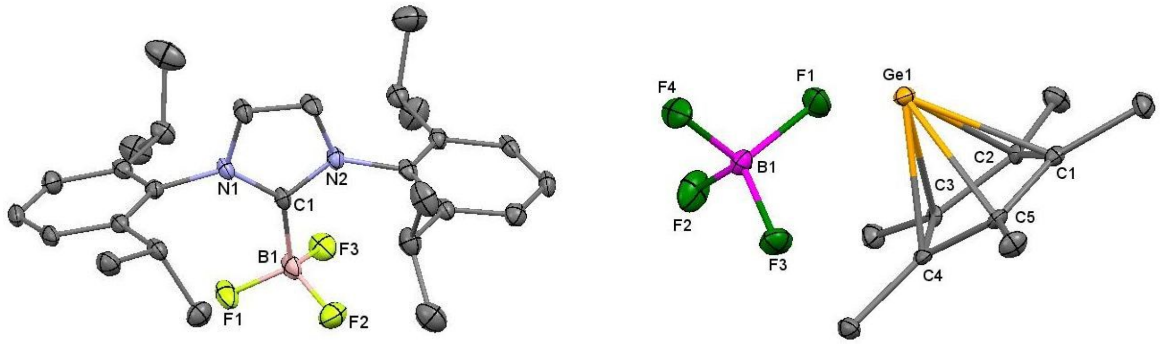

Figure S8. The molecular structure of **11** and **13** (ellipsoids are shown at the probability level of 30%). Hydrogen atoms are omitted for clarity.

S5. References

S1. (a) S. S. Sen, J. Hey, R. Herbst-Irmer, H. W. Roesky and D. Stalke, *J. Am. Chem. Soc.,* **2011**, *133*, 12311–12316. (b) S. S. Sen, M. P. Kritzler-Kosch, S. Nagendran, H. W. Roesky, T. Beck, A. Pal and R. Herbst-Irmer, *Eur. J. Inorg. Chem.*, **2010**, 5304–5311. (c) P. P. Samuel, A. P. Singh, S. P. Sarish, J. Matussek, I. Objartel, H. W. Roesky and D. Stalke, *Inorg. Chem.*, 2013, ***52***, 1544−1549. (d) S. Khan, S. S. Sen, H. W. Roesky, D. Kratzert, R. Michel and D. Stalke, *Inorg. Chem.* 2010, ***49***, 9689–9693.

S2. P. Jutzi, F. Kohl, P. Hofmann, C. Krüger and Y.-H. Tsay, *Chem. Ber.* **1980**, 113, 757 – 769.

S3. C. Pranckevicius and D. W. Stephan, *Chem. Eur. J.* **2014**, 20, 6597 – 6602.

S4. (a) A. D. Becke*, Phys. Rev. A* **1988**, *38*, 3098 - 3100. (b) J. P. Perdew, *Phys. Rev. B* **1986**, *33*, 8822 – 8824.

S5. M. J. Frisch, G. W. Trucks, H. B. Schlegel, G. E. Scuseria, M. A. Robb, J. R. Cheeseman, G. Scalmani, V. Barone, B. Mennucci, G. A. Petersson, H. Nakatsuji, M. Caricato, X. Li, H. P. Hratchian, A. F. Izmaylov, J. Bloino, G. Zheng, J. L. Sonnenberg, M. Hada, M. Ehara, K. Toyota, R. Fukuda, J. Hasegawa, M. Ishida, T. Nakajima, Y. Honda, O. Kitao, H. Nakai, T. Vreven, J. A. Montgomery,.Jr., J. E .Peralta, F. Ogliaro, M. Bearpark, J. J. Heyd, E. Brothers, K. N. Kudin, V. N. Staroverov, T. Keith, R. Kobayashi, J. Normand, K. Raghavachari, A. Rendell, J. C. Burant, S. S. Iyengar, J. Tomasi, M. Cossi, N. Rega, J. M. Millam, M. Klene, J. E. Knox, J. B. Cross, V. Bakken, C. Adamo, J. Jaramillo, R. Gomperts, R. E. Stratmann, O. Yazyev, A. J. Austin, R. Cammi, C. Pomelli, J. W. Ochterski, R. L. Martin, K. Morokuma, V. G. Zakrzewski, G. A. Voth,

P. Salvador, J. J. Dannenberg, S. Dapprich, A. D. Daniels, O. Farkas, J. B. Foresman, J. V. Ortiz, J. Cioslowski and D. J. Fox, Gaussian, Inc., Wallingford CT, **2010**.

S6. F. Weigend, R. Ahlrichs, *Phys. Chem. Chem. Phys*. **2005**, *7*, 3297 – 3305

S7. Y. Zhao, D. G. Truhlar, *Theor. Chem. Acc*. **2008**, *120*, 215 - 241.

S8. (a) A. E. Reed, L. A. Curtiss, F. Weinhold, *Chem. Rev.* **1988**, *88*, 899 – 926. (b) NBO 6.0. E. D. Glendening, J. K. Badenhoop, A. E. Reed, J. E. Carpenter, J. A. Bohmann, C. M. Morales, C. R. Landis, F. Weinhold (Theoretical Chemistry Institute, University of Wisconsin, Madison, WI, **2013**); http://nbo6.chem.wisc.edu/. (c) E. D. Glendening, C. R. Landis, F. Weinhold, *WIREs Comput. Mol. Sci.* **2012**, *2*, 1 – 42

S9. (a) S. R. Gadre, *J. Chem. Phys.*, **1992**, 96, 5253 – 5260. (b). G. Naray-Szabo, G. Ferenczy, *Chem. Rev.* **1995**, *95*, 829. (c). R. N. Shirsat, S. V. Bapat, S. R. Gadre, *Chem. Phys. Lett.* **1992**, *200*, 373.

S10. (a) T. Lu, F. Chen, *J. Comput. Chem.*, **2012**, *33*, 580 – 592; (b) T. Lu, F. Chen, *J. Mol. Graphics Modell.*, **2012**, *38*, 314 – 323.

S11. a) K. Morokuma, *J. Chem. Phys.* **1971**, *55*, 1236 - 1244; b) T. Zeigler, A. Rauk, *Inorg. Chem.* **1979**, *18*, 1755 - 1759; c) Zeigler, A. Rauk, *Inorg. Chem.* **1979**, *18*, 1558 - 1565; c) M. v. Hopffgarten, G. Frenking, *WIREs Comput. Mol. Sci.* **2012**, *2*, 43 - 62.

S12. (a) J. G. Snijders, P. Vernoojs, E. J. Baerends, *At. Data Nucl. Data Tables* **1981**, *26*, 483 - 509. (b) G. te Velde, F. M. Bickelhaupt, E. J. Baerends, C. F. Guerra, S. J. A. v. Gisbergen, J. G. Snijders, T. Ziegler, *J. Comput. Chem.* **2001**, *22*, 931 - 967. (c) C. F. Guerra, J. G. Snijders, G. te Velde, E. J. Baerends, *Theor. Chem. Acc.* **1998**, *99*, 391 - 403. (d) ADF **2016**, SCM, Theoretical Chemistry, Vrije Universiteit, Amsterdam, The Netherlands, http://www.scm.com.

S13. (a) A. Michalak, M. Mitoraj, T. Zeigler, *J. Phys. Chem. A* **2008**, *112*, 1933 - 1939; (b) M. Mitoraj, A. Michalak, *Organometallics* **2007**, *26*, 6576 - 6580; (c) M. Mitoraj, A. Michalak, *J. Mol. Model* **2007**, *13*, 347 - 355; (d) M. Mitoraj, A. Michalak, *J. Mol. Model* **2008**, *14*, 681 - 687; (d) M. P. Mitoraj, A. Michalak and T. Ziegler, *J. Chem. Theory Comput.* **2009**, *5*, 962 - 975; (e) M. Mousavi and G. Frenking, *Organometallics*, **2013**, *32*, 1743-1751; (f) T. A. N. Nguyen and G. Frenking, *Chem. Eur. J.*, **2012**, 18, 12733-12748.

S6. NMR Spectra

^{1}H, ^{13}C, ^{29}Si, ^{11}B, ^{31}P, ^{119}Sn and ^{19}F NMR spectrum of 3, 4, 5, 6, 8, 10 and 12:

Figure S9: ^{1}H NMR (400.31 MHz, CDCl$_3$) of compound **3**

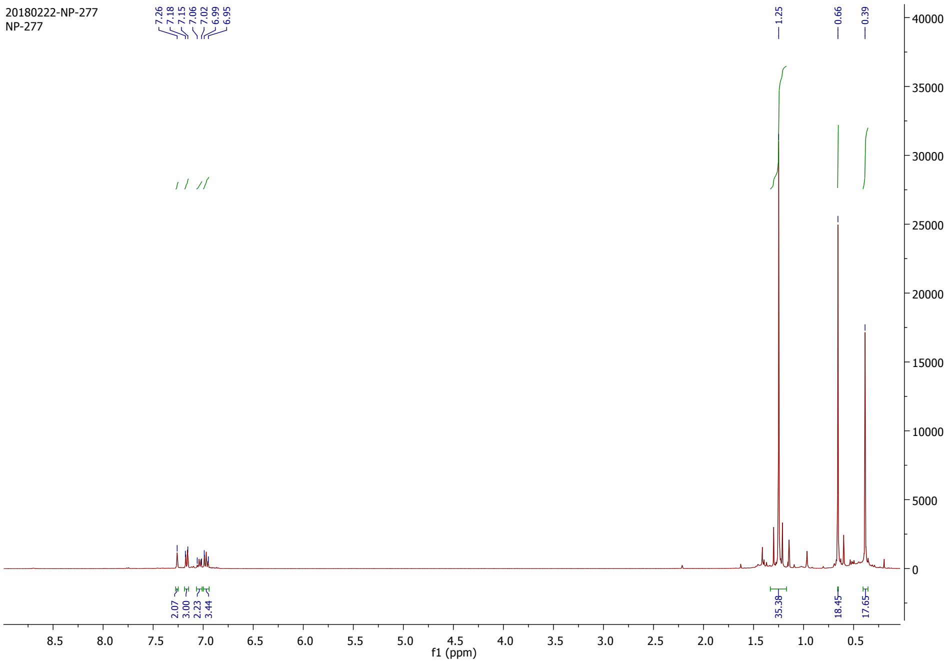

Figure S10: ^{19}F NMR (376.49 MHz, CDCl$_3$) of compound **3**

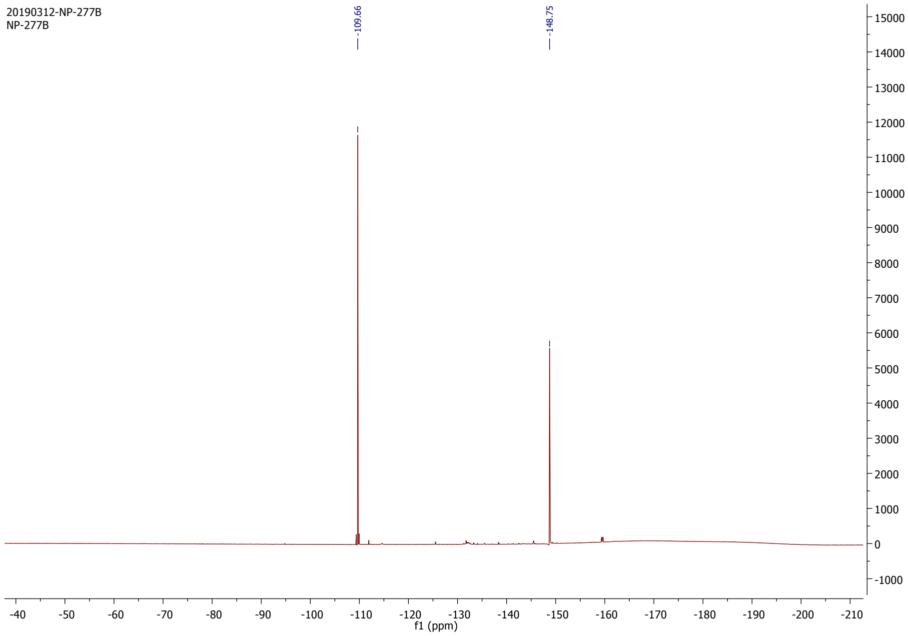

Figure S11: ^{13}C NMR (100.613 MHz, CDCl$_3$) of compound **3**

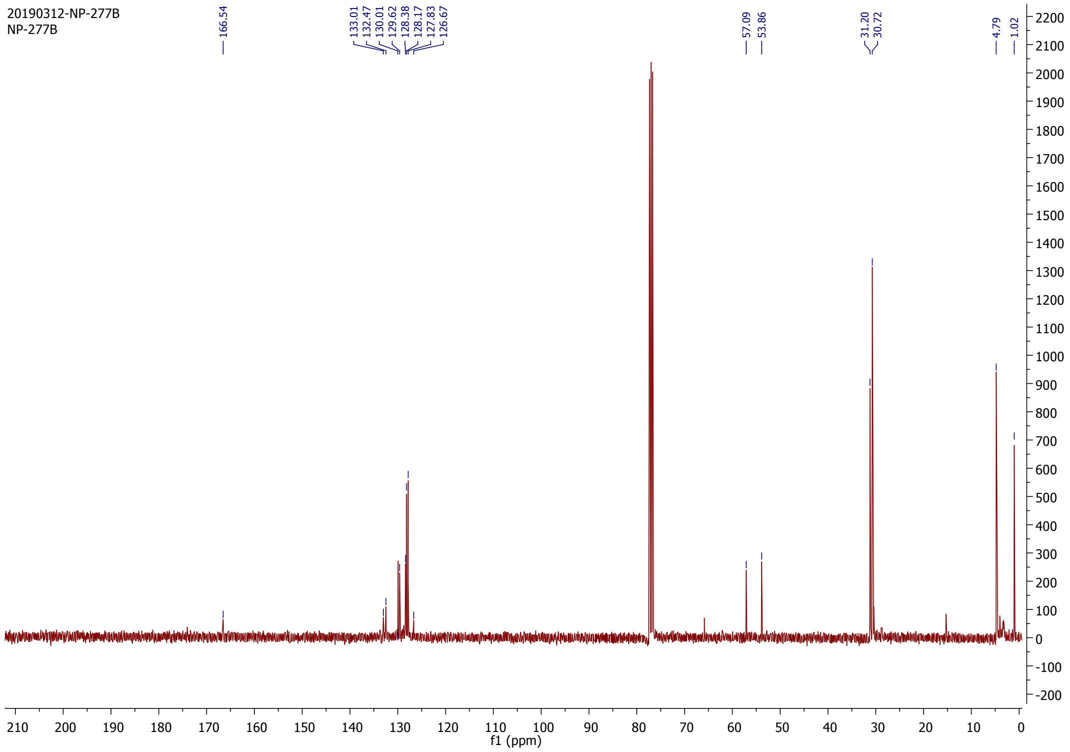

Figure S12: ^{11}B NMR (128.387 MHz, CDCl$_3$) of compound **3**

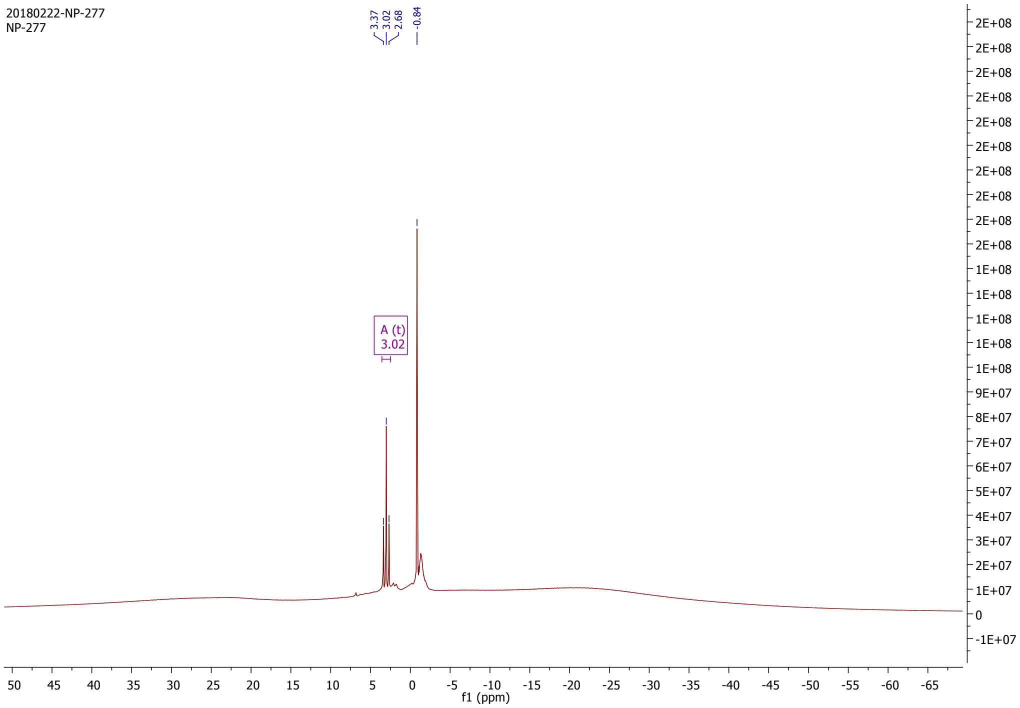

Figure S13: ^{29}Si NMR (79.495 MHz, CDCl$_3$) of compound **3**

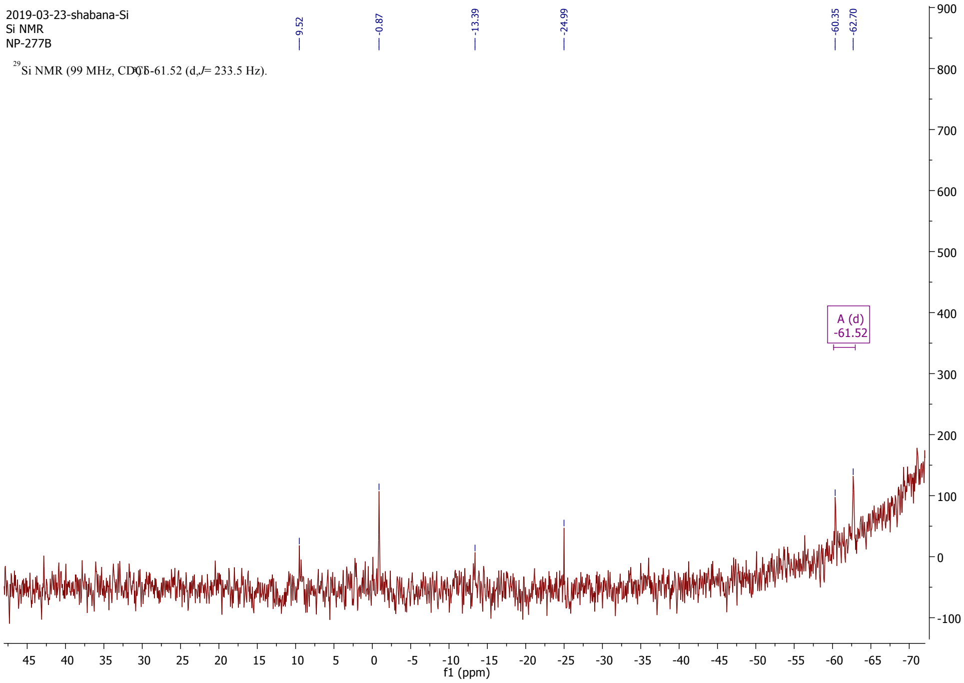

Figure S14: ^{1}H NMR (400.31 MHz, CDCl$_3$) of compound **5**

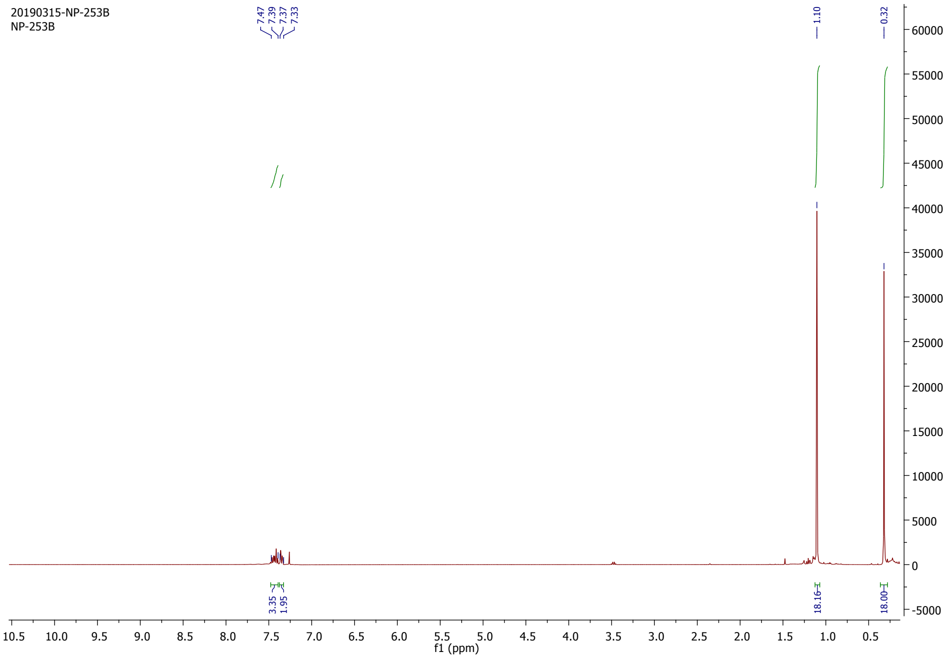

Figure S15: ^{13}C NMR (100.613 MHz, $CDCl_3$) of compound **5**

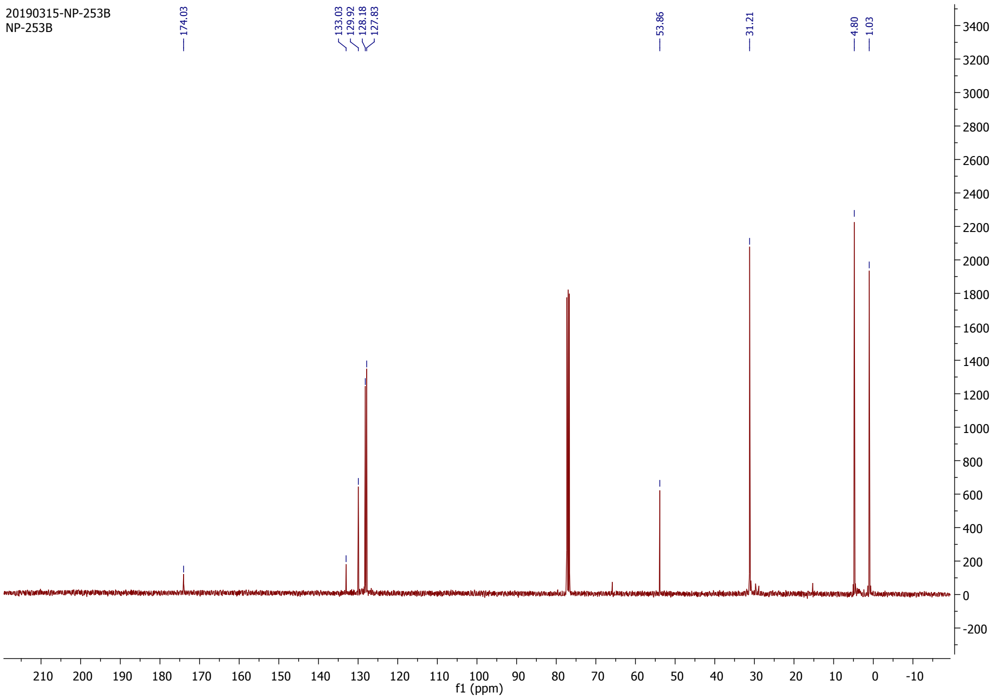

Figure S16: ^{19}F NMR (376.49 MHz, $CDCl_3$) of compound **5**

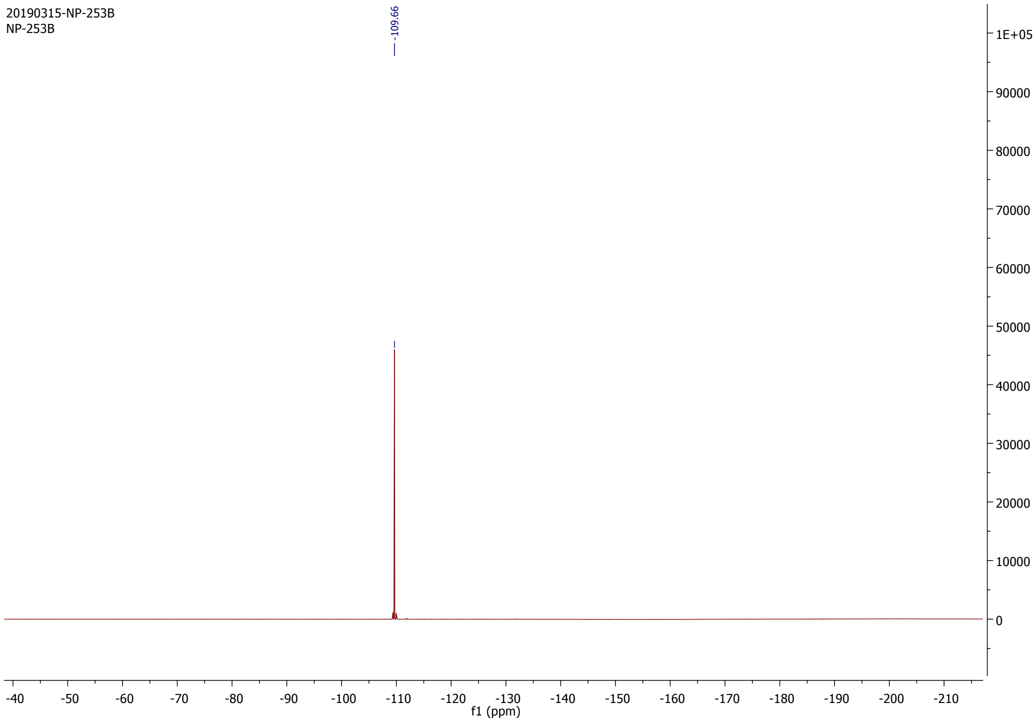

Figure S17: ^{1}H NMR (400.31 MHz, CDCl$_3$) of compound **4**

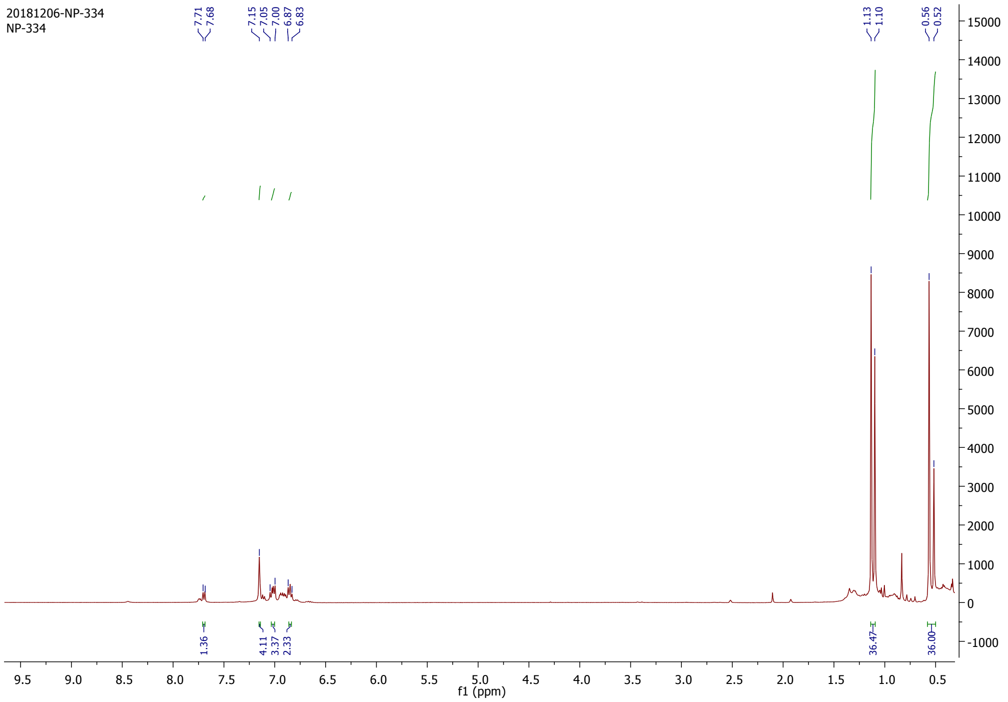

Figure S18: ^{13}C NMR (100.613 MHz, CDCl$_3$) of compound **4**

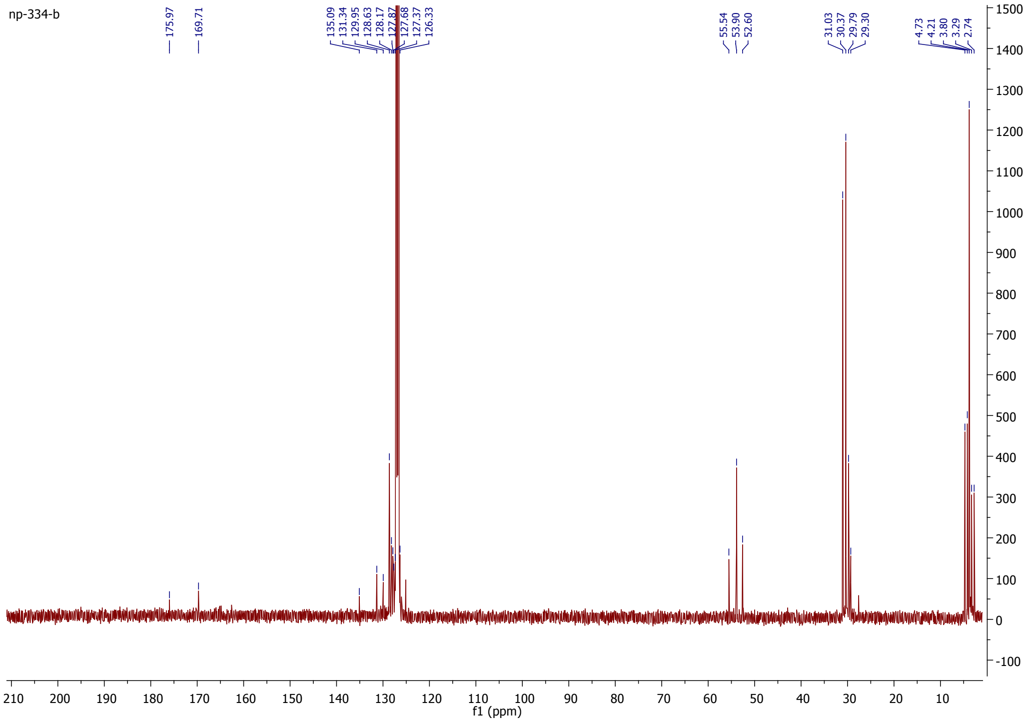

Figure S19: ^{19}F NMR (376.49 MHz, $CDCl_3$) of compound **4**

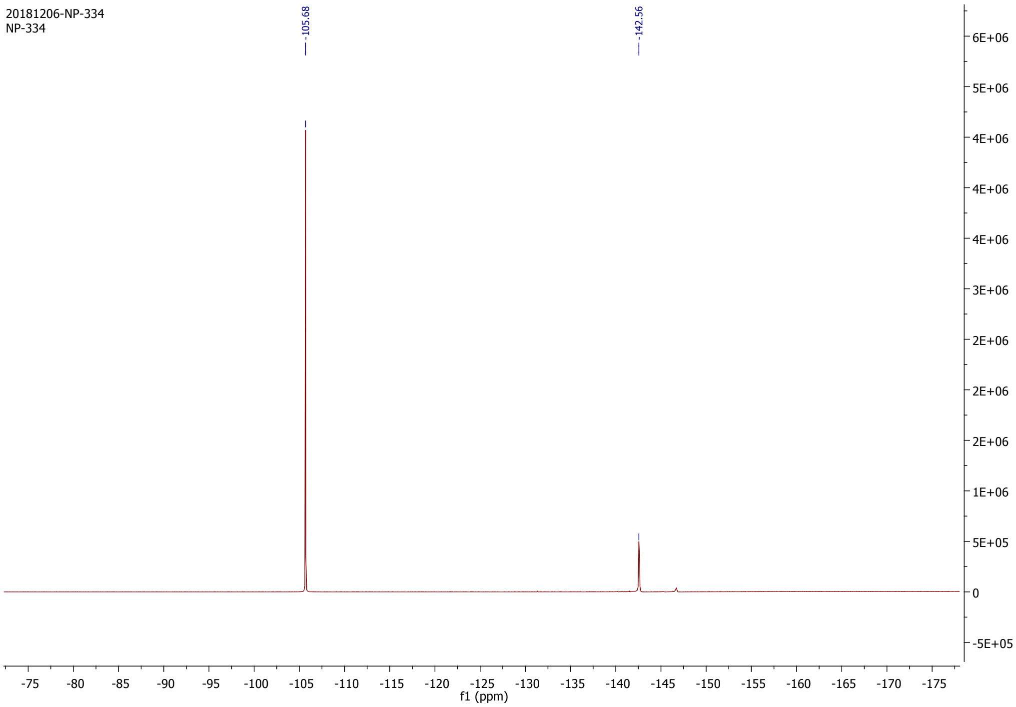

Figure S20: ^{29}Si NMR (79.495 MHz, $CDCl_3$) of compound **4**

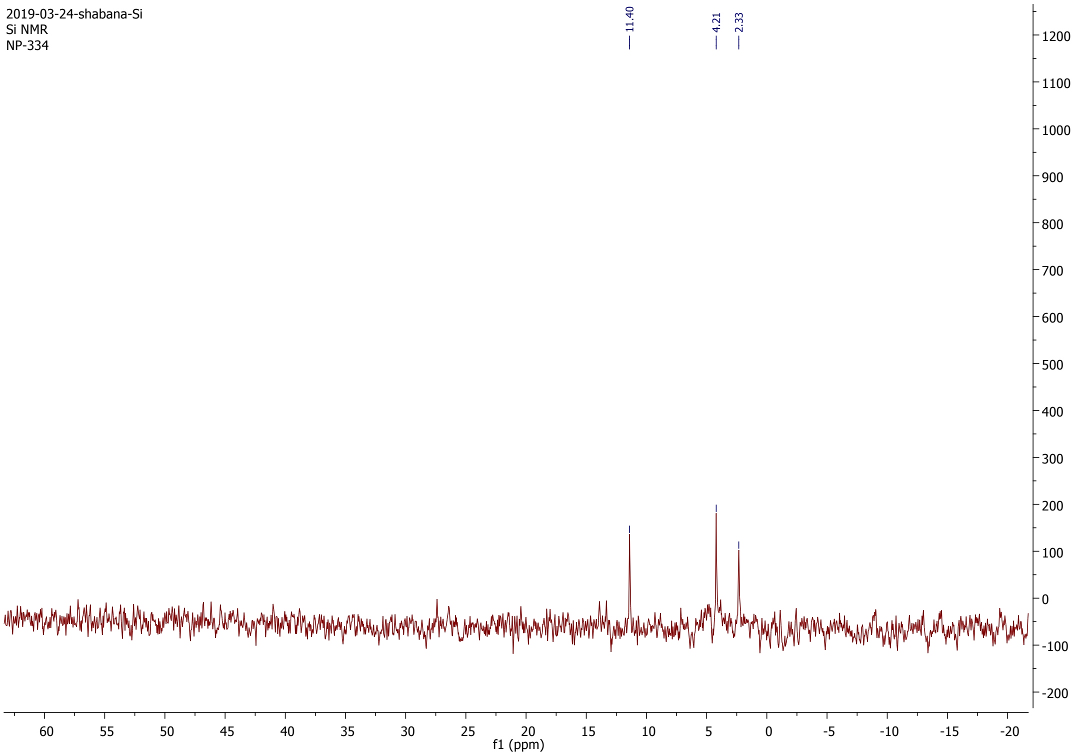

Figure S21: ^{11}B NMR (128.387 MHz, CDCl$_3$) of compound **4**

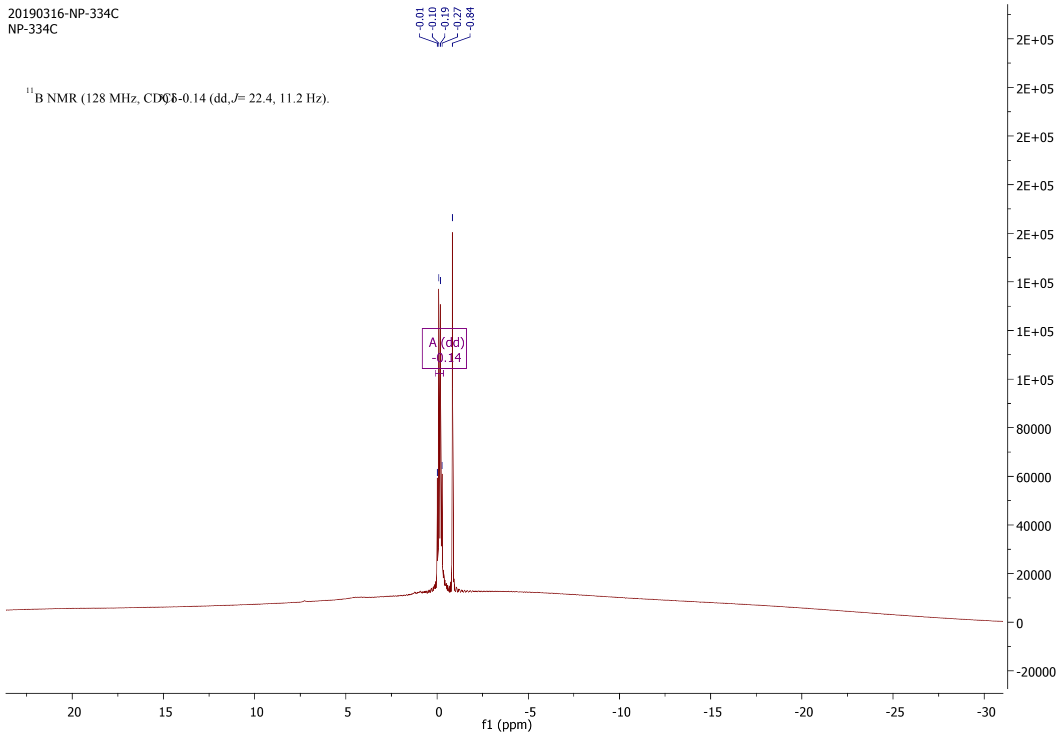

Figure S22: ^{1}H NMR (400.31 MHz, CDCl$_3$) of compound **6**

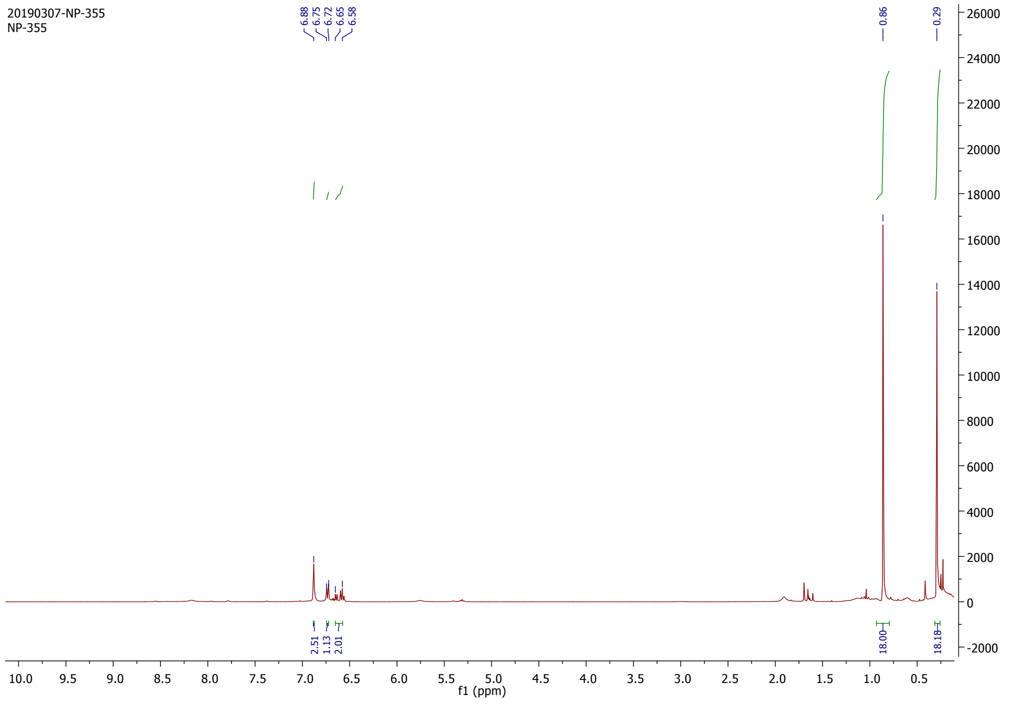

Figure S23: ^{19}F NMR (376.49 MHz, CDCl$_3$) of compound **6**

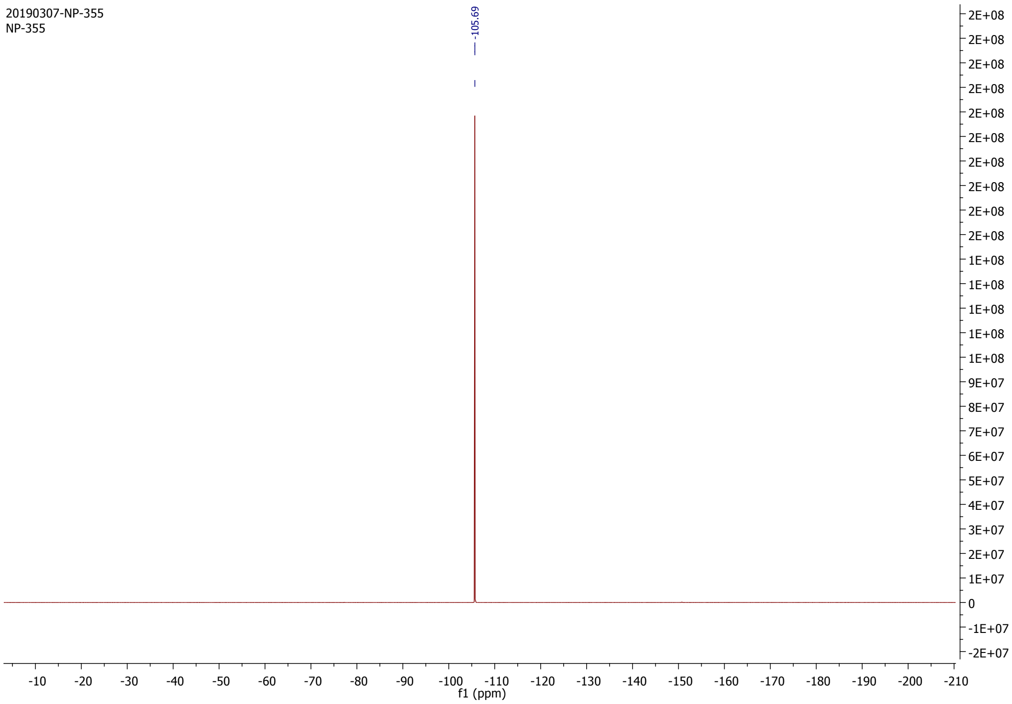

Figure S24: ^{1}H NMR (400.31 MHz, CDCl$_3$) of compound **8**

(*= grease peak)

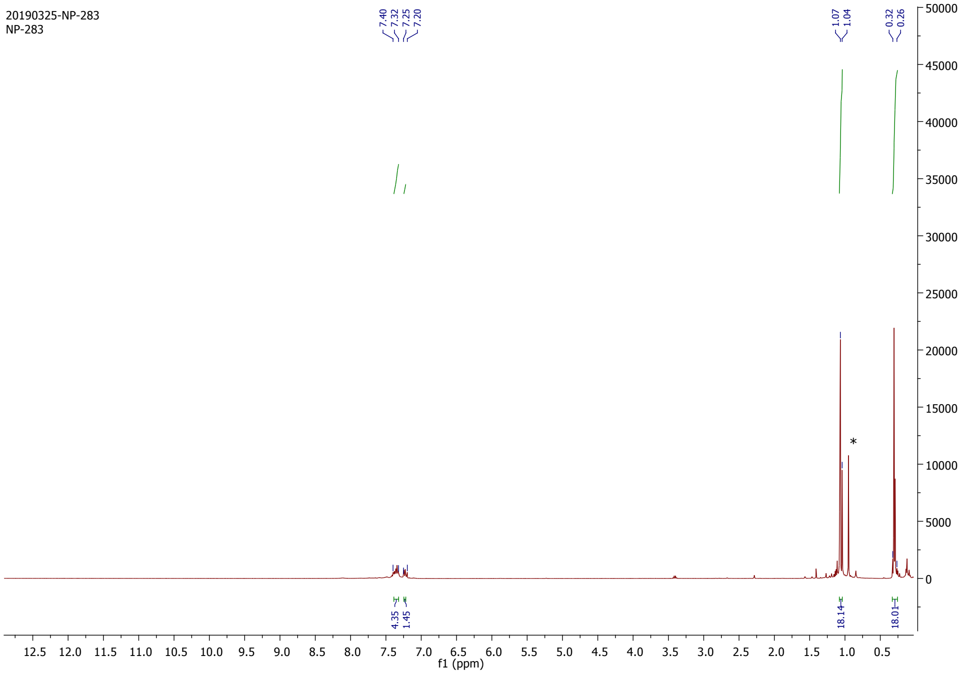

Figure S25: ^{13}C NMR (100.613 MHz, CDCl$_3$) of compound **8**

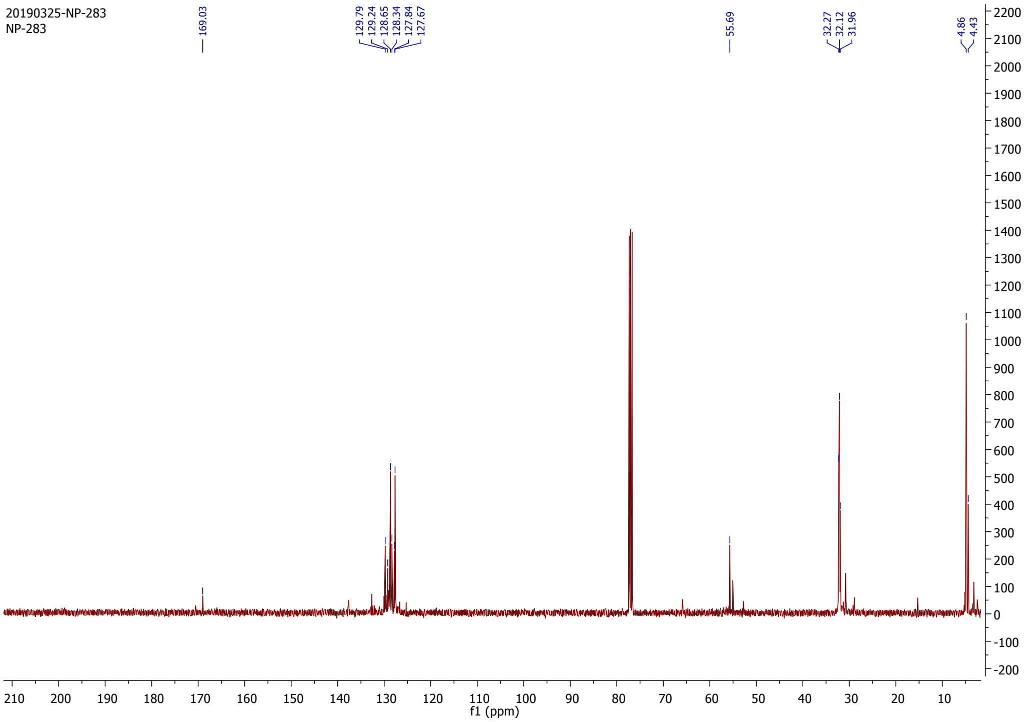

Figure S26: ^{19}F NMR (376.49 MHz, CDCl$_3$) of compound **8**

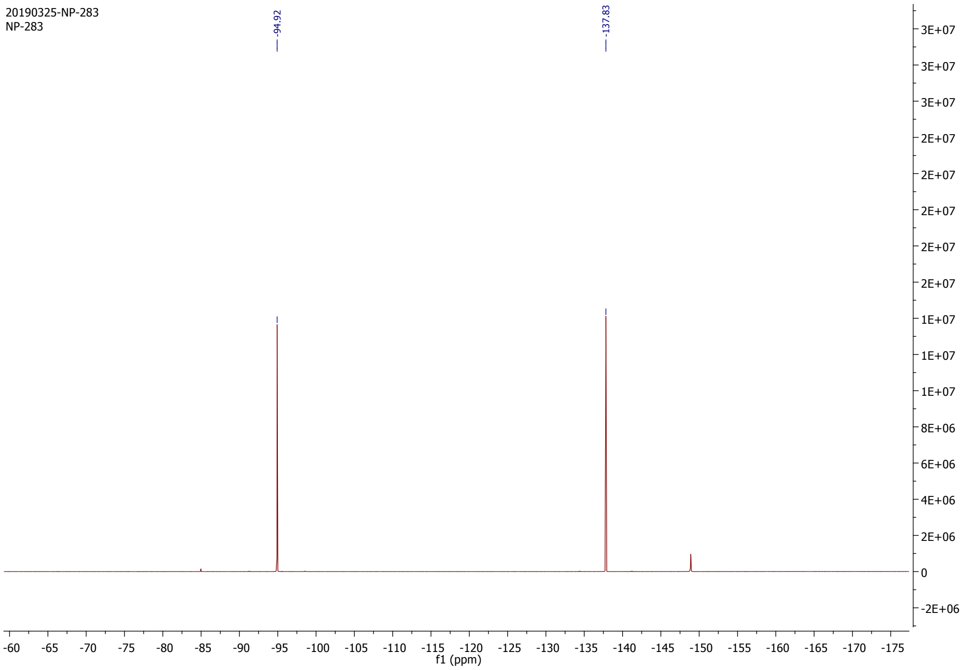

Figure S27: ^{29}Si NMR (79.495 MHz, $CDCl_3$) of compound **8**

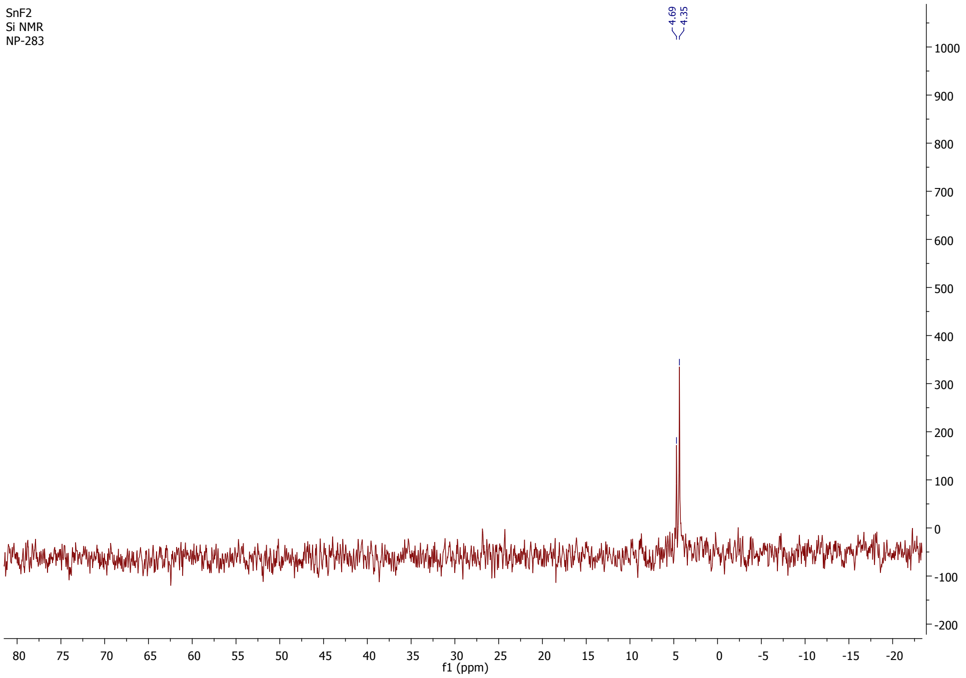

Figure S28: ^{119}Sn NMR (149.18 MHz, $CDCl_3$) of compound **8**

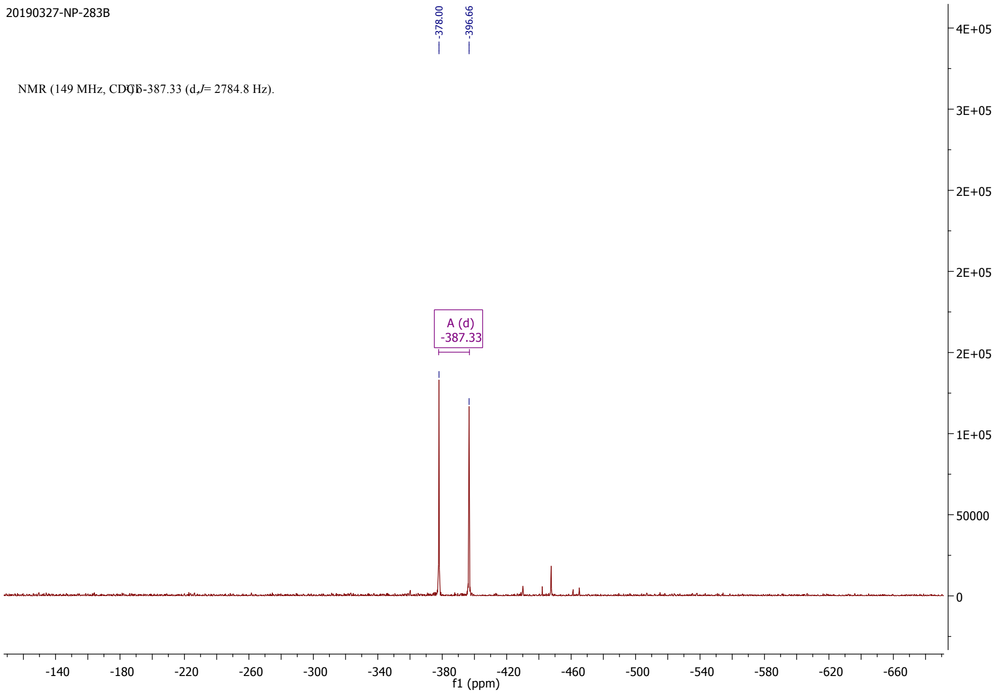

Figure S29: ^{1}H NMR (400.31 MHz, CDCl$_3$) of compound **10**

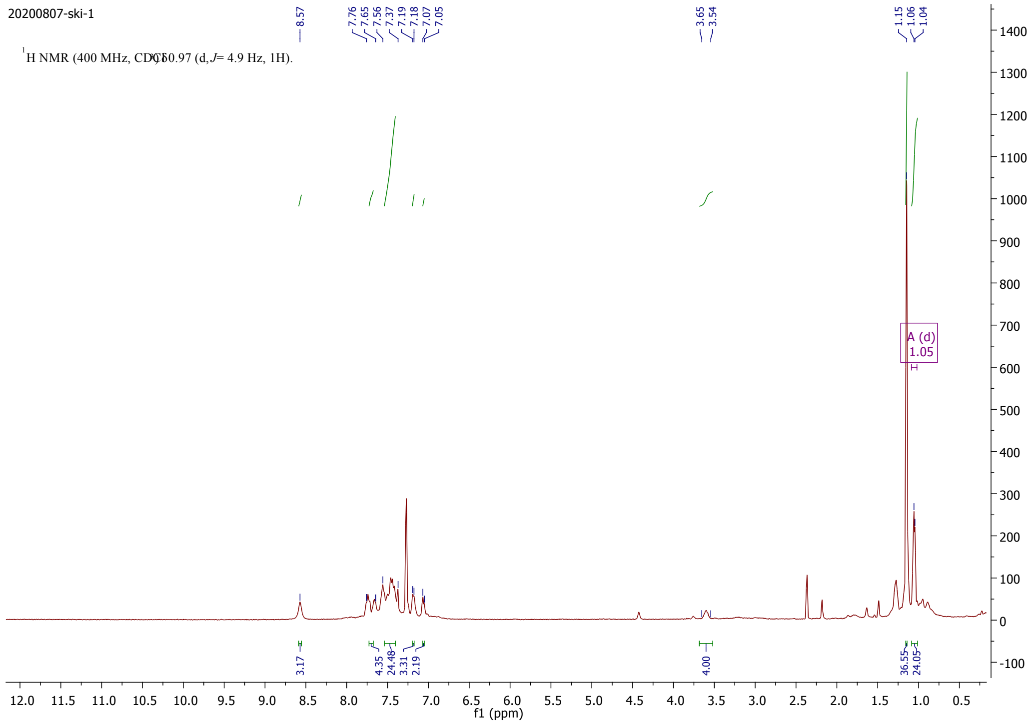

Figure S30: ^{13}C NMR (100.613 MHz, CDCl$_3$) of compound **10**

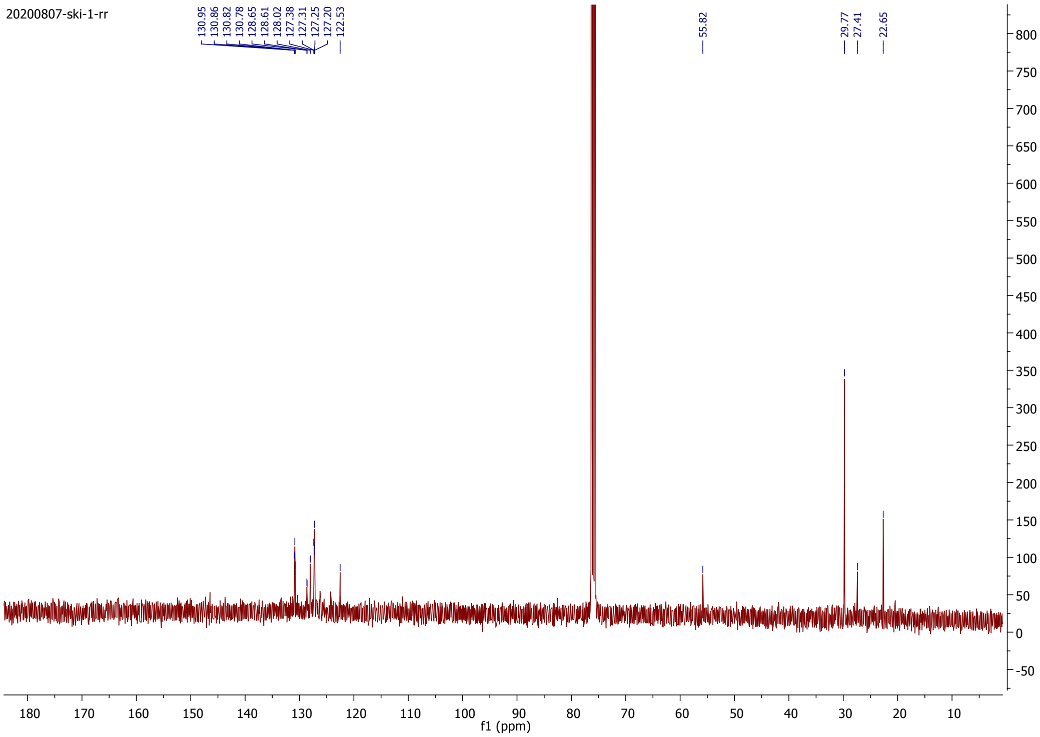

Figure S31: ^{11}B NMR (128.387 MHz, CDCl$_3$) of compound **10**

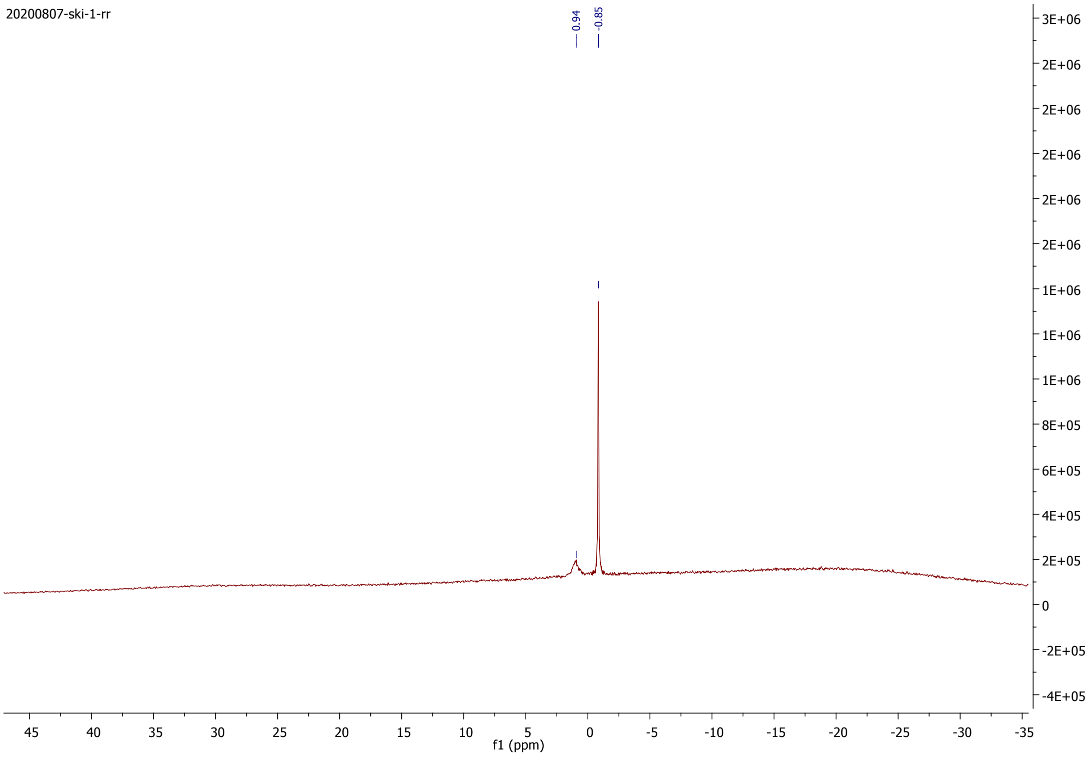

Figure S32: ^{19}F NMR (376.49 MHz, CDCl$_3$) of compound **10**

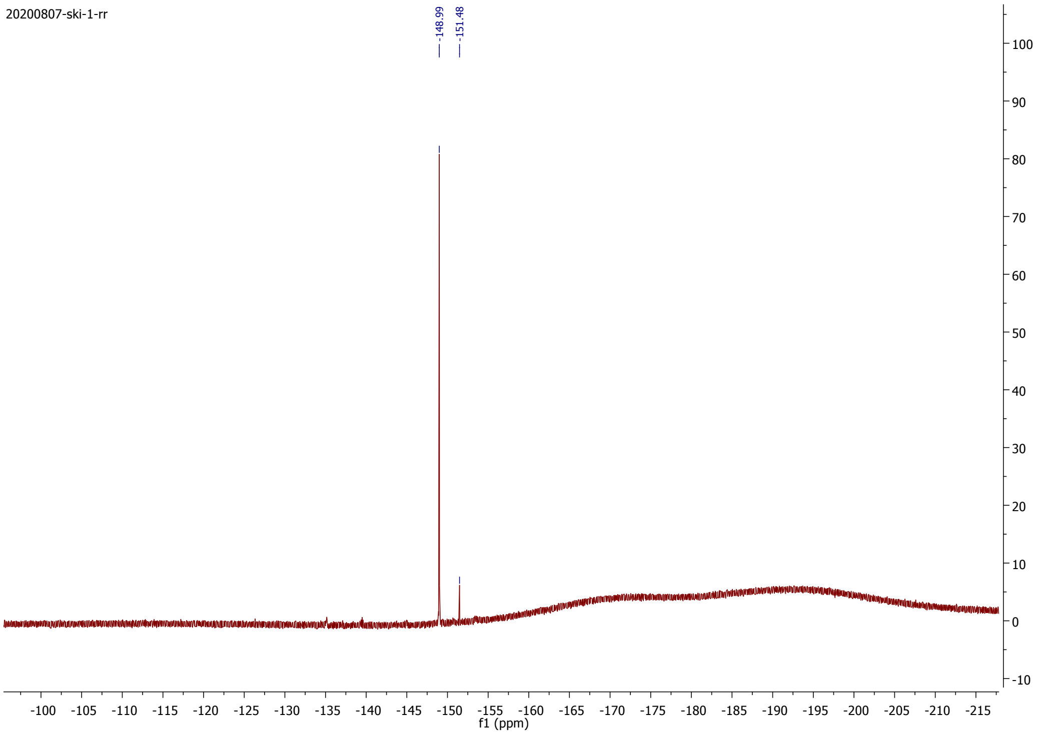

Figure S33: ^{31}P NMR (161.97 MHz, $CDCl_3$) of compound **10**

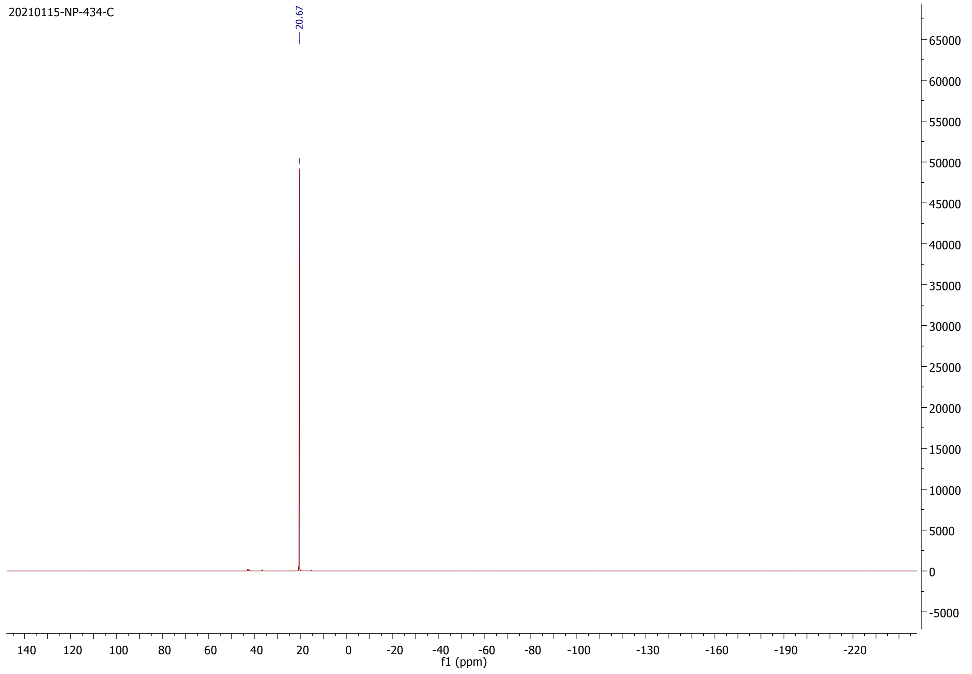

Figure S34: ^{119}Sn NMR (149.18 MHz, $CDCl_3$) of compound **10**

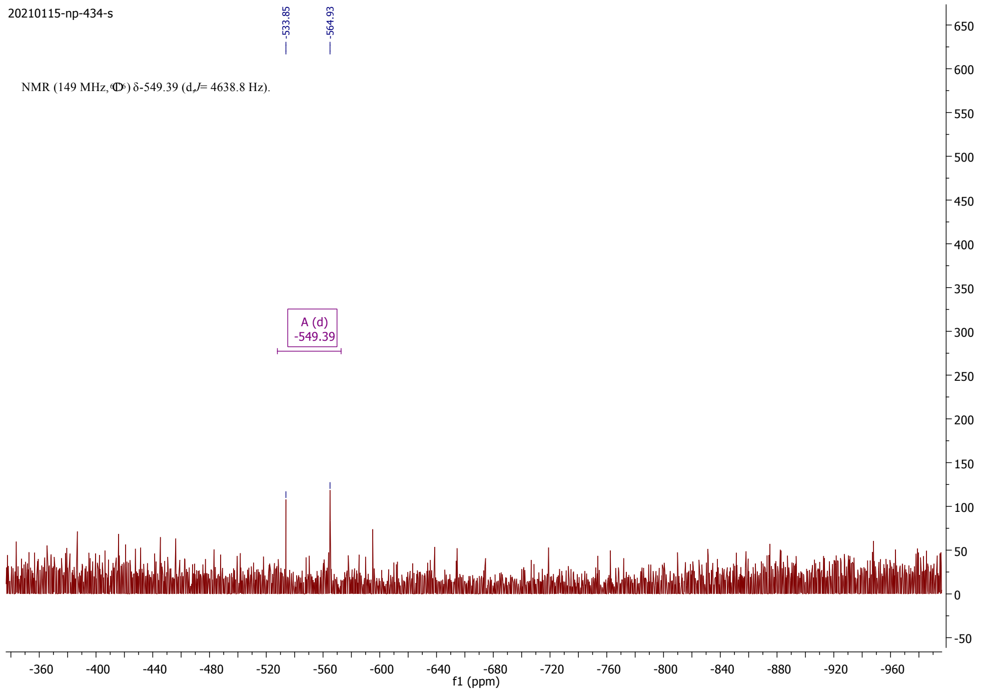

Figure S35: ^{19}F NMR (376.49 MHz, CDCl$_3$) of compound **12**

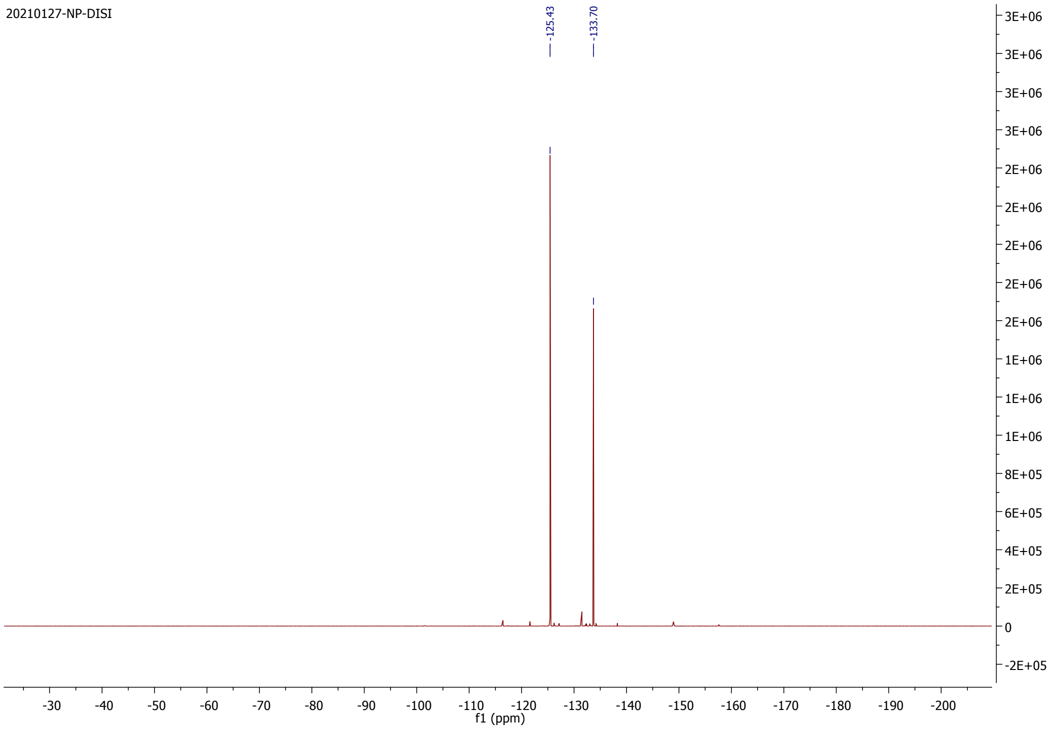

Figure S36: ^{29}Si NMR (79.495 MHz, CDCl$_3$) of compound **12**